

Justus-Liebig-Universität Gießen
Faculty 09 Agricultural Sciences, Nutritional Sciences and Environmental Management
Institute of Landscape Ecology and Resources Management
Professorship of Resources Management

Construction and specification of a cryogenic vacuum extraction device for application in stable water isotope analysis

Master-Thesis in Environmental and Resources Management
Module: MKU 31: Quantitative Landscape Analysis

Supervisors: PD Dr. Lutz Breuer
Prof. Dr. Hans-Georg Frede
Submitted by: B.Sc. Natalie Orlowski
Address: Friedensstr. 10
35394 Gießen
07/05/2010

Eidesstattliche Erklärung

Ich versichere, dass ich die vorliegende Arbeit selbständig verfasst und keine anderen als die angegebenen Hilfsmittel verwendet habe. Ich versichere weiterhin, dass die Stellen, die anderen Werken wörtlich oder sinngemäß entnommen sind, als solche kenntlich gemacht sind und die Arbeit in gleicher oder ähnlicher Fassung noch nicht Bestandteil einer Studien- oder Prüfungsleistung war.

Gießen, den

Natalie Orłowski

Acknowledgement

I would like to express my gratitude to Prof. Dr. Frede for the possibility to write my M.Sc. Thesis at his institute. Further appreciation goes to my advisor Dr. Breuer, who always supported and helped me friendly. In addition, I would like to thank Mr. Köstler, who assisted me with his technical expertise and Mr. Julich, who performed the stable water isotope analysis.

Natalie Orlowski

Gießen, May 2010

I. Table of Contents

I. TABLE OF CONTENTS	4
II. INDEX OF FIGURES	5
III. INDEX OF TABLES	7
1. INTRODUCTION	8
1.1 Stable water isotopes	9
1.1.1 Definitions and Terminology	9
1.1.2 History and Standards	10
1.1.3 Isotope fractionation.....	13
1.1.4 Application of stable water isotopes	21
1.2 Hydrogen and oxygen isotope analysis	25
1.2.1 Mass spectrometry.....	25
1.2.2 Diode laser absorption spectroscopy	26
1.3 Soil and plant water extraction methods for isotopic water analysis	28
1.3.1 Azeotropic distillation	28
1.3.2 Centrifugation.....	29
1.3.3 Cryogenic vacuum extraction.....	30
2. MATERIALS AND METHODS.....	37
2.1 Material selection and technical description	37
2.2 Procedure of cryogenic vacuum extraction	44
2.3 Validation experiments	47
2.4 Analytic measuring method for stable water isotopes	50
3. RESULTS AND DISCUSSION	52
3.1 Impact test on the extracted water isotope signature.....	53
3.2 Effect of the high-purity nitrogen aeration.....	56
3.3 Cross-contamination test among the extraction units	61
4. CONCLUDING REMARKS AND OUTLOOK.....	64
5. ABSTRACT	66
6. ZUSAMMENFASSUNG.....	68
7. REFERENCES	70
8. APPENDIX.....	75
8.1 Appendix 1	75
8.2 Appendix 2	82

II. Index of figures

Figure 1: The relationship between $\delta^{18}\text{O}$ and $\delta^2\text{H}$ values defined by the GMWL.....	13
Figure 2: Equilibrium fractionation factors α for the isotope ratios $^2\text{H}/^1\text{H}$ and $^{18}\text{O}/^{16}\text{O}$ as a function of temperature [$^{\circ}\text{C}$]	16
Figure 3: Rainout effect on $\delta^2\text{H}$ and $\delta^{18}\text{O}$ values	19
Figure 4: Seasonal variation in $\delta^{18}\text{O}$ in precipitation at stations from low to high latitude in North America.....	20
Figure 5: The altitude effect on local rainfall in the Italian Alps.....	21
Figure 6: Isotopic composition of C and O pools in the carbon and water cycles.....	22
Figure 7: Time course of the hydrogen isotope ratio of xylem sap in eastern white pine (<i>Pinus strobus</i>) following a summer rain event.....	23
Figure 8: Depth/ δ value relationship for steady-state evaporation from a saturated sand column.....	24
Figure 9: Essential components of a gas isotope mass spectrometer with Dual Inlet system for reference and sample material.....	25
Figure 10: A typical GC/MS system diagram.....	26
Figure 11: Principle of Tunable Diode Laser Absorption Spectroscopy	27
Figure 12: Azeotropic distillation apparatus for soil-water extraction	29
Figure 13: A) Centrifuge extraction tube and B) Filter adapter composition	30
Figure 14: Schematic of equipment used to extract soil water.	31
Figure 15: Schematic of a cryogenic extraction line.....	31
Figure 16: Schematic and photography of the device for extracting water from soils and plants of the ISIRF.....	33
Figure 17: Photography of cryogenic vacuum extraction device for soil and plant material of the PSI.....	34
Figure 18: Apparatus for the batch distillation of plant stem-water samples.....	35
Figure 19: Schematic of the whole vacuum extraction device at the ILR	39
Figure 20: Schematic of the whole vacuum distribution system	40
Figure 21: Photography and schematic of one extraction unit.....	41
Figure 22: Schematic of an extraction-collection unit and its angular connection tube	42
Figure 23: Photography of the ILR's cryogenic vacuum extraction device	43

Figure 24: A) Schematic of one extraction unit with its extraction-collecktio unit. B) Close-up photography of the extraction-collection units with their angular connection tubes C) Close-up photography of the extraction tubes including soil samples fixed with fleece	45
Figure 25: LGR DLT-100-Liquid Water Isotope Analyser	50
Figure 26: Functional principal of the LGR DLT-100.....	51
Figure 27: Comparison of the $\delta^2\text{H}$ values of Gießen's tap water before and after water extraction without high-purity nitrogen aeration	54
Figure 28: Comparison of the $\delta^{18}\text{O}$ values of Gießen's tap water before and after water extraction without high-purity nitrogen aeration	54
Figure 29: Comparison of the $\delta^2\text{H}$ values of Gießen's tap water after water extraction with and without high-purity nitrogen aeration.....	57
Figure 30: Comparison of the $\delta^{18}\text{O}$ values of Gießen's tap water after water extraction with and without high-purity nitrogen aeration.....	57
Figure 31: Comparison of the $\delta^2\text{H}$ values of Schwingbach water before and after water extraction with high-purity nitrogen aeration.....	59
Figure 32: Comparison of the $\delta^{18}\text{O}$ values of Schwingbach water before and after water extraction with high-purity nitrogen aeration.....	60
Figure 33: Comparison of the $\delta^2\text{H}$ values of precipitation from Gießen and Schwingbach water after the same water extraction procedure with high-purity nitrogen aeration	62
Figure 34: Comparison of the $\delta^{18}\text{O}$ values of precipitation from Gießen and Schwingbach water after the same water extraction procedure with high-purity nitrogen aeration	63
Figure 35: Photography of fiver extraction unit used at the PSI.....	65

III. Index of tables

Table 1: Average terrestrial abundances of the stable water isotopes.....	10
Table 2: Characteristic physical properties of the three major water isotopes.....	13
Table 3: Investigating issues of the validation experiments	48
Table 4: Descriptive statistics of the $\delta^2\text{H}$ and $\delta^{18}\text{O}$ values of Gießen's tap water before and after water extraction for validation experiment 1	53
Table 5: Descriptive statistics of the $\delta^2\text{H}$ and $\delta^{18}\text{O}$ values [‰] with/without high-purity nitrogen aeration for validation experiment 2.1	56
Table 6: Descriptive statistics of the $\delta^2\text{H}$ and $\delta^{18}\text{O}$ values of Schwingbach water before and after water extraction with high-purity nitrogen aeration for validation experiment 2.2.....	59
Table 7: Descriptive statistics of the $\delta^2\text{H}$ and $\delta^{18}\text{O}$ values of precipitation from Gießen and Schwingbach water after water extraction for validation experiment 3.....	62
Table 8: Material list	75
Table 9: Raw data of validation experiment 1	82
Table 10: Raw data of validation experiment 2.1	83
Table 11: Raw data of validation experiment 2.2	84
Table 12: Raw data of validation experiment 3	85

1. Introduction

Stable isotopes of water - particularly ^1H and ^2H as well as ^{16}O and ^{18}O - can assist in the solution of hydrogeochemical and biological problems due to their natural and overall existence in water cycles (Clark and Fritz, 1997). They improve the understanding of the origin, formation, and flow path of water and, therefore, provide insights across a range of spatial scales from the cell to the plant community, ecosystem, region or global and over temporal scales (Dawson et al., 2002). Thereby, physicochemical differences, determined by the dissimilar numbers of neutrons and, therefore, by different masses of the stable water isotopes, lead to different chemical behaviours of isotopes in the environment. This phenomenon is called isotope fractionation (Unkovich et al., 2001). This different behaviour in physical and chemical reactions is the major reason that in nature stable water isotopes exist in different ratios and can consequently be used as natural tracers. The differences in isotope ratios are expressed relatively to an international standard in per mil [‰] (Aggarwal et al., 2007).

However, to determine the isotopic signature of environmental water, it is necessary to separate the water from the other components of the sample media (plant material, soil). Therefore, several extraction methods have been developed: Azeotropic distillation, cryogenic vacuum extraction, and centrifugation. Cryogenic vacuum extraction is one of the most widely used methods to obtain extracts suitable for isotopic water analysis (Peters and Yakir, 2008). Hence, the aim of this thesis was to construct a vacuum-tight, reliable, and user-friendly cryogenic vacuum extraction device with an extendable modularity and several independently working extraction units for the application in stable water isotope research sciences in order to extract water from soil and plant samples and, thereafter, analyse their stable water isotope composition to quantify hydrological processes in local water cycles.

After studying the existing cryogenic vacuum extraction devices, decisions for the construction of a new extraction apparatus at the Institute of Landscape Ecology and Resources Management (ILR) were made according to which parts of the existing devices could be adopted, which materials could be chosen, and which components could be improved. However, the main concern of the new cryogenic vacuum extraction device was to have an absolutely vacuum-tight system providing a complete water extraction from the samples accompanying by no changes in the isotopic composition of the samples. An additional concern was to construct a device with independent extraction units in order to have the possibility to extract only one sample, to minimise evaporation, i. e. a modified isotopic composition of the extracted water after the extraction procedure, and, thus, to reduce the probability of error. To consider these

issues the apparatus was equipped with six independent extraction units, each with a mechanism for high-purity nitrogen aeration. Nitrogen gas is an inert gas and does not react with the stable isotopes of water and, can therefore, be used as an aeration gas serving as a kind of protective layer above the extracted water to minimise evaporative water loss, which would affect the water isotopic signature.

After the construction of the apparatus, the new vacuum extraction device has to be specified through validation experiments. The aim of the validation experiments was to test whether the water isotopic signature is changed through the extraction process, whether the high-purity nitrogen aeration affects the water isotopic composition, and whether cross-contamination among the six extraction units occurs leading to mixed sample waters and changed isotopic signatures.

1.1 Stable water isotopes

1.1.1 Definitions and Terminology

Isotopes of an element have different atomic masses due to the varying numbers of neutrons (Unkovich et al., 2001). The mass number is noted as the superscript number on the left of the element designation. Furthermore, it can generally be distinguished between stable and radioactive isotopes. A so called stable isotope does not decay to other isotopes on geologic time scales, but may itself be produced by the decay of radioactive isotopes (Kendall and McDonnell, 1998). In opposite to stable isotopes, unstable ones show radioactive decay of the atomic nucleus. The building parts of water, hydrogen and oxygen, have both stable and unstable isotopes. Hydrogen has two stable isotopes: ^1H (protium) and ^2H (deuterium) and oxygen has three stable isotopes: ^{16}O , ^{17}O , ^{18}O . Whereas, in nature only three of the nine stable isotopic different water molecules occur in easily measurable concentrations: $^1\text{H}_2^{16}\text{O}$, $^1\text{H}_2^{18}\text{O}$, $^1\text{H}^2\text{H}^{16}\text{O}$ (Araguas-Araguas et al., 2000). The stable isotopes of most elements are composed of one major abundant isotope and one or two isotopes with minor abundance. The low abundance of these isotopes provides opportunities to use enriched sources of these isotopes as tracers in environmental studies (Unkovich et al., 2001). Table 1 shows the average terrestrial abundances of the stable water isotopes.

Table 1: Average terrestrial abundances of the stable water isotopes (Rundel et al., 1989; modified).

Element	Isotope	Abundance [%]
Hydrogen	¹ H	99.985
	² H	0.015
Oxygen	¹⁶ O	99.759
	¹⁷ O	0.037
	¹⁸ O	0.204

The isotopic composition of a natural sample is expressed as δ notation relatively to an international standard in per mil [‰]:

$$\delta = \frac{(R_{\text{sample}} - R_{\text{standard}})}{R_{\text{standard}}} \times 1000 \text{ [‰]} \quad \text{Eq. 1}$$

(Aggarwal et al., 2007)

R denotes the ratio of the heavy to light isotope (e. g., ²H/¹H; ¹⁸O/¹⁶O) in atomic percent. R_{sample} and R_{standard} are the ratios in sample and standard, respectively. A positive δ value means that the isotopic ratio of the sample is higher than that of the standard; a negative δ value expresses the opposite case (Kendall and McDonnell, 1998).

1.1.2 History and Standards

According to Aggarwal et al. (2007) the primary criterion for a reference standard is that it should represent a major pool of a given element under consideration. In 1953 “average ocean water” was proposed and used as reference standard for water isotopic measurements. However, at that time no “average ocean water” existed. Hence, Craig (1961b) constituted the hypothetical Standard Mean Ocean Water (SMOW) as zero-point of that conventional scale in terms of real reference water. This reference was established by mixing different seawater compartments (Atlantic, Pacific, and Indian Ocean) according to the weighted average isotope ratio existing at that time as a reference. Even this concept (SMOW) was based on a hypothetical approach and not a real water sample was available as a reference standard. Therefore, SMOW could not be used directly to calibrate laboratory measurements. For that reason, an International Atomic Agency (IAEA) panel of experts suggested in 1966 that two new wa-

ter reference materials were necessary. One standard should be as close as possible to the Craig's SMOW (1961b) and the other should serve as reference for highly depleted waters – with an abundance of the heavier water isotopes - close to the lowest limits observed in natural waters. The new “SMOW” was prepared by mixing distilled ocean water with small amounts of other waters by R. Weiss and H. Craig. The second standard, the so called “Standard Light Antarctic Precipitation” (SLAP), was created by melting a firm sample from Plateau Station, Antarctica, by E. Picciotto (Aggarwal et al., 2007). The following analysis showed that the new SMOW had the same $^{18}\text{O}/^{16}\text{O}$ ratio, but a slightly different $\delta^2\text{H}$ ratio (-0.2 [‰]) as the hypothetical SMOW, which can be neglected in practice, because most laboratories have a higher measurement uncertainty than this discrepancy (Aggarwal et al., 2007).

Results of the new SMOW analysis (VSMOW):

$$\left(\frac{\text{O}^{18}}{\text{O}^{16}}\right)_{\text{VSMOW}} = (2005.2 \pm 0.45) \times 10^{-6} \quad \text{Eq. 2}$$

(Baertschi, 1976)

$$\left(\frac{\text{H}^2}{\text{H}^1}\right)_{\text{VSMOW}} = (155.76 \pm 0.05) \times 10^{-6} \quad \text{Eq. 3}$$

(Hagemann et al., 1970)

The relation between the two standards is expressed as follows:

$$\delta^{18}\text{O}_{\text{SLAP}} = -55.5 \text{ [‰] VSMOW} \quad \text{Eq. 4}$$

$$\delta^2\text{H}_{\text{SLAP}} = -428.0 \text{ [‰] VSMOW} \quad \text{Eq. 5}$$

(Clark and Fritz, 1997)

Unfortunately, the new and old SMOW had the same name in the beginning, until the IAEA decided to rename the new SMOW in “Vienna Standard Mean Ocean Water” (VSMOW) to make a difference between the old hypothetical and the new real water reference standard. In 1976, an IAEA Consults' Meeting determined that all future water isotope ratios should be reported as $\delta^2\text{H}$ and $\delta^{18}\text{O}$ values relative to VSMOW (Aggarwal et al, 2007).

The first analysis of non-marine meteoric water (i. e. the atmospheric moisture, the precipitation, the ground-, and the surface water derived from them) samples by Epstein and Mayeda (1953) and Friedman (1953) showed that there was a linear correlation between the hydrogen and oxygen isotope ratios. Subsequently, Craig (1961a) analysed around four hundred samples of river and lake water, rain, and snow from different parts of the world. He discovered that the water isotope ratios of these samples – except for those from the lakes – could be expressed by the following equation:

$$\delta^2H = 8 \delta^{18}O + 10 \quad \text{Eq. 6}$$

This equation became known later as the “global meteoric water line” (GMWL), which traced the isotopic compositions of natural waters, originating from atmospheric precipitation and not subjected to surface evaporation (Aggarwal et al., 2007). Generally, the GMWL provides a reference for the comparison of local differences in water and, thus, for interpreting the origin of waters (University of Kwazulu-Natal, Geography seminar, 2003). The value of ten in this equation differs significantly from area to area and over geological age.

When the local $\delta^{18}O$ and δ^2H values of precipitation are plotted relatively to each other, this linear relation is called “Local Meteoric Water Line” (LMWL). For example, the LMWL in arid environments will have the same slope as the GMWL, but plot higher in relation to δ^2H because of increased evaporation in these regions. Likewise, LMWLs of humid environments maintain the slope of eight, but their line shifts towards increased $\delta^{18}O$ because the phase change tends towards liquid precipitation (SAHRA, 2010). For instance, a value greater than + 24 [‰] for the Mediterranean region is reported by Cook and Herczeg (2000).

Even today, the isotopic signature of precipitation is recorded by the “Global Network of Isotopes in Precipitation” (GNIP), which is located at the IAEA Headquarter in Vienna. Since 1961, Rozanski et al. (1993) have revised the GMWL equation slightly through the use of the IAEA’s global sampling network GNIP and detected:

$$\delta^2H = 8.13 \delta^{18}O + 10.8 \quad \text{Eq. 7}$$

The linear correlation between the $\delta^{18}O$ and δ^2H values of precipitation, defined by the GMWL, is shown in Figure 1. The general trend of the GMWL is that the waters of cold regions tend to be isotopically depleted relatively to the waters of warm regions.

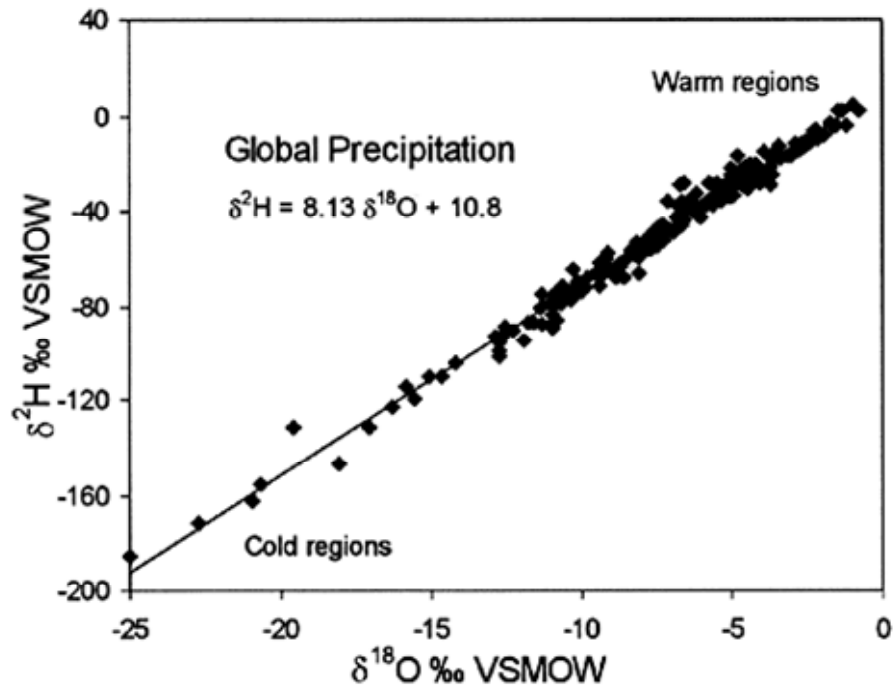


Figure 1: The relationship between $\delta^{18}\text{O}$ and $\delta^2\text{H}$ values defined by the GMWL (SAHRA, 2010).

1.1.3 Isotope fractionation

Physicochemical differences, determined by the dissimilar numbers of neutrons and, therefore, by different masses, lead to different chemical behaviours of isotopes. The different physical properties of the three major water isotopes are shown in Table 2. H_2^{16}O is the most common form of water on earth.

Table 2: Characteristic physical properties of the three major water isotopes (Unkovich et al., 2001; modified).

Property	H_2^{16}O	$^2\text{H}_2^{16}\text{O}$	H_2^{18}O
Density [20°C; $\text{kg}\cdot\text{m}^{-3}$]	910	1110	1110
Temperature of greatest density [°C]	3.98	11.24	4.30
Melting point [101 kPa; °C]	0.00	3.81	0.28
Boiling point [101 kPa; °C]	100.00	101.42	100.14
Vapour pressure [100°C; kPa]	101	96	101

This different behaviour in chemical reactions is the major reason for the different δ values of isotopes. The process that causes different isotope ratios is called isotope fractionation. The following aspects are caused by isotope mass differences:

- a)** The heavier isotopic molecules have a lower mobility. The kinetic energy of a molecule is determined mostly by temperature:

$$kT = \frac{m \cdot v^2}{2} \quad [\text{J}] \quad \text{Eq. 8}$$

In the equation k denotes the Boltzmann constant [J/K], T the absolute temperature [K], m the molecular mass [kg], and v the average molecular velocity [$\text{m}\cdot\text{s}^{-1}$]. This means that the molecules with larger masses have a smaller molecular velocity. The consequences of this fact are: heavier molecules have a lower diffusion velocity and their collision frequency with other molecules is smaller - the primary condition for chemical reaction. That is why light molecules react faster than heavy ones.

- b)** Thermodynamically, the oscillation energy of the heavy isotopes bonds is lower than the one of light isotopes and, therefore, they are more stable than light isotopes. According to this fact, light isotopes need lower activation energy. Consequently, the hydrogen bridges of $^{18}\text{O}^1\text{H}$ are stronger than the hydrogen bridges of $^{16}\text{O}^1\text{H}$.

These circumstances induce isotope fractionation. The isotopic composition of an element in a certain compound changes the transition of the compound from one physical state or chemical composition to another (IAEA, 2010a). Isotope fractionation can mathematically be described by comparing the isotope ratios of the two compounds in a chemical equilibrium ($A \leftrightarrow B$) or of the compounds before and after a physical or chemical transition process ($A \rightarrow B$). The isotope fractionation is quantified by the isotope fractionation factor α , which is then defined as the ratio of the two isotopes, which expresses the isotope ratio in the phase or compound B relative to that in A:

$$\alpha_{A(B)} = \alpha_{\frac{B}{A}} = \frac{R(B)}{R(A)} = \frac{R_B}{R_A} \quad \text{Eq. 9}$$

Generally, isotope effects are approximately $\alpha \approx 1$. Therefore, the variation of α from 1 is used more often than the fractionation factor. This variable is defined by:

$$\varepsilon_{B/A} = \alpha_{B/A} - 1 = \frac{R_B}{R_A} - 1 \quad \text{Eq. 10}$$

Whereat, ε stands for the enrichment ($\varepsilon > 0$) or the depletion ($\varepsilon < 0$) of the rare isotope in B with respect to A. The symbols $\alpha_{B/A}$ and $\varepsilon_{B/A}$ correspond to $\alpha_{A(B)}$ and $\varepsilon_{A(B)}$. In the one-way process ($A \rightarrow B$) ε is the change in isotopic composition, i.e. the new isotopic composition compared to the old (IAEA, 2010a).

In general, there are three different kinds of mass-dependent isotope fractionation: the **kinetic** fractionation, the **equilibrium** fractionation, and the **transport** fractionation. Kinetic fractionation is caused by irreversible (one-way physical or chemical) processes. It is a measure of the differences in kinetic energy, exhibited between a light and heavy isotope. Transport fractionation is a special case of isotope fractionation, which is affected by irreversible physical processes, but differs from kinetic fractionation. It occurs due to the different mobilities of the isotopic species of water, such as $^1\text{H}_2^{16}\text{O}$, $^1\text{H}_2^{18}\text{O}$, $^1\text{H}^2\text{H}^{16}\text{O}$ (IAEA, 2010b). The equilibrium (or thermodynamic) fractionation is basically the isotope effect participated in a thermodynamic isotopic equilibrium reaction, meaning the forward and backward reaction rates of any particular isotope are identical. As an equilibrium reaction the isotope exchange reaction is chosen:



The asterisks indicate the presence of the rare isotope (^2H or ^{18}O). The equilibrium isotope fractionation factor α is defined for the equilibrium between phases A and B by the equilibrium constant K of this exchange reaction:

$$K(T) = \frac{[A][^*B]}{[^*A][B]} = \frac{[^*B]/[B]}{[^*A]/[A]} = \frac{R_B}{R_A} = \alpha_{B/A}(T) \quad \text{Eq. 12}$$

(IAEA, 2010a).

In this equation, R is the ratio of the abundance of the particular isotope species. The equivalent expression for the equilibrium constant is the isotope fractionation factor α corresponding to the one in equation 9 and 10, respectively.

The equilibrium isotope effect depends on many factors, of which temperature (T) is generally the most important:

$$\frac{R_{(phase1)}}{R_{(phase2)}} = \alpha_{1/2}(T) \quad \text{Eq. 13}$$

(IAEA, 2010b).

Equilibrium fractionation factors as a function of temperature are shown for the stable isotopes of water in Figure 2. As can be seen, the fractionation factor α is higher for ^2H than for ^{18}O and inversely related to the temperature. For this reason isotope fractionation increases with the mass difference and decreases with higher temperatures (Seiler and Gat, 2007).

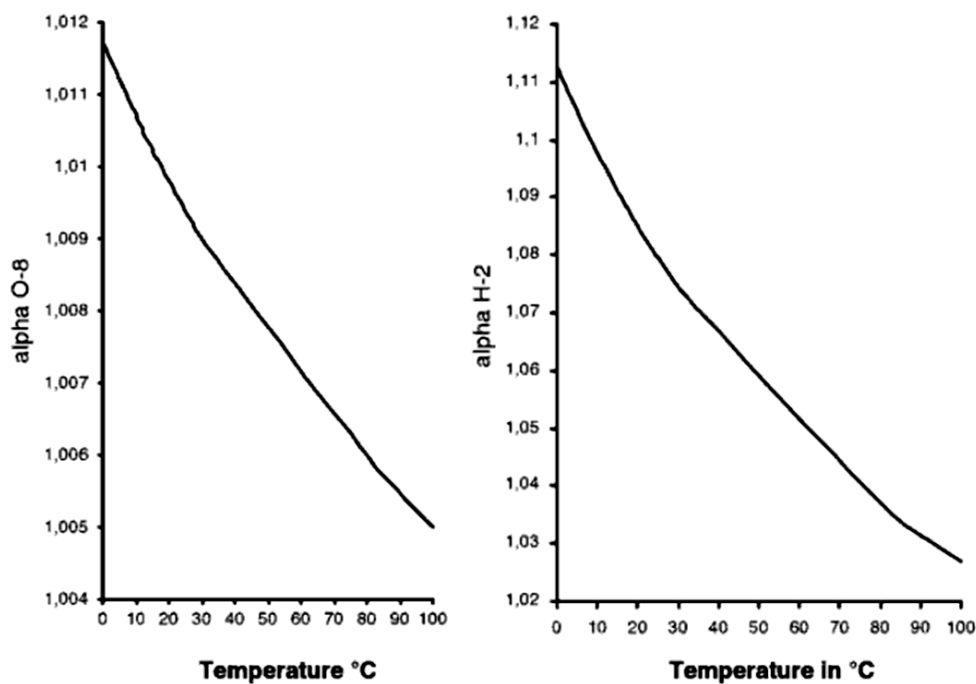


Figure 2: Equilibrium fractionation factors α for the isotope ratios $^2\text{H}/^1\text{H}$ and $^{18}\text{O}/^{16}\text{O}$ as a function of temperature [°C] (Seiler and Gat, 2007).

As a rule, among different phases of the same compound or different species of the same element, the denser the material or the larger the compound's molecular mass, the more it tends to be enriched in the heavier isotope. For example, for the various phases of water at equilibrium: $\delta^{18}\text{O}_{\text{Solid}} > \delta^{18}\text{O}_{\text{Liquid}} > \delta^{18}\text{O}_{\text{Vapour}}$ (IAEA, 2010b).

In one-way or irreversible chemical or biochemical reactions, the isotope fractionation factor is designated as α_{kin} to distinguish it from equilibrium fractionation factor $\alpha_{1/2}$ in equation 13.

According to this definition, α_{kin} is smaller than one (and ϵ_{kin} negative), if the actual process causes a depletion and α_{kin} is bigger than one (ϵ_{kin} positive), in case of an enrichment of the rare isotopes (^2H or ^{18}O) (IAEA, 2010b). When kinetic fractionation occurs, the phase or compound that is formed is depleted in the heavy isotope with respect to the original phase or compound (k smaller than one).

However, an additional difficulty arises, since in nature the processes are not simply kinetic or irreversible. Moreover, kinetic fractionation is difficult to measure in the laboratory, because complete irreversibility cannot be guaranteed (part of the water vapour will return to the liquid) and the exact degree of irreversibility cannot be quantified. It can be established that water is depleted in ^{18}O compared to the original water, when it evaporates fast. Isotope fractionation processes, which are not only kinetic (one-way processes), will be referred to as non-equilibrium fractionations. For example, evaporation can take place under more or less equilibrium conditions: at 100% humidity, still air, and an almost chemically closed system. However, generally, the system is not in chemical equilibrium, e. g. smaller than 100% humidity or the products become partially isolated from the reactants, for example, when the resultant vapour is blown downwind (Kendall and McDonnell, 1998). Under these conditions, the equilibrium is affected by an additional kinetic isotope effect. Further, evaporation of ocean or fresh surface water bodies is neither a one-way (kinetic) process nor an equilibrium process.

Moreover, the fractionation due to kinetic isotope effects generally exceeds that from equilibrium processes. The reason for this is that principally an equilibrium process consists of two opposite one-directional processes. Furthermore, in a kinetic process, the formed compound may be depleted in the rare isotopes (^2H or ^{18}O) while it is enriched in the equivalent equilibrium process (IAEA, 2010a).

Transport isotope fractionation is a special case of kinetic fractionation. It appears in two cases: first when a part of a system is removed by a chemical or biological reaction and second when material escapes by diffusion or outflow (IAEA, 2010b). In the first reaction, the mass difference between the isotopic molecules, as described above, plays a major role. In the second reaction, a gas kinetic process is involved, where fractionation arises from the differences in the diffusive velocities between isotopes. Therefore, the transport fractionation is also called diffusive fractionation. During the diffusion into a vacuum, the equilibrium fractionation is the ratio of the velocities of the two isotopes. For this fractionation factor, equation 8 - converted to v - and equation 10 have to be combined:

$$\alpha_{m^*/m} = \frac{v^*}{v} = \frac{\sqrt{\frac{kT}{2m^*}}}{\sqrt{\frac{kT}{2m}}} = \sqrt{\frac{m}{m^*}} \quad \text{Eq. 14}$$

Here v^* and v mark the average molecular velocities [$\text{m}\cdot\text{s}^{-1}$] of the two gases or solutes, k the Boltzmann constant (gas constant per molecule), m^* and m the molecular masses [kg], and T the absolute temperature [$^{\circ}\text{C}$] (Clark and Fritz, 1997).

However, where a gas or solute is diffusing through another medium, the mass of the medium (in this case: air) must be taken into consideration, using the following fractionation factor:

$$\alpha = \left[\frac{m^*(m + 28.8)}{m(m^* + 28.8)} \right]^{\frac{1}{2}} \quad \text{Eq. 15}$$

In this equation m^* and m represent the molecule mass of the two diffusive gases and 28.8 is the average mass of air (79 % N_2 , and 21 % O_2 ; i.e. $0.79 \times 28 + 0.21 \times 32 = 28.8$) (Clark and Fritz, 1997).

The combination of all fractionation processes induces the following effects:

1.) Continental/ rainout effect:

Precipitation isotope δ values decrease (more negative values) towards continental interior (University of Utah, Isotope course, 2009). After evaporation of water vapour from the ocean, the vapour moves in clouds towards inland, condenses, and rains out over the continent. As a result, this rainfall is isotopically enriched compared to the water vapour. The more the water vapour moves inland (the distance to the ocean increases) the more the δ values decrease. In addition, the rainfall is progressively depleted with increasing distance from the ocean (Figure 3).

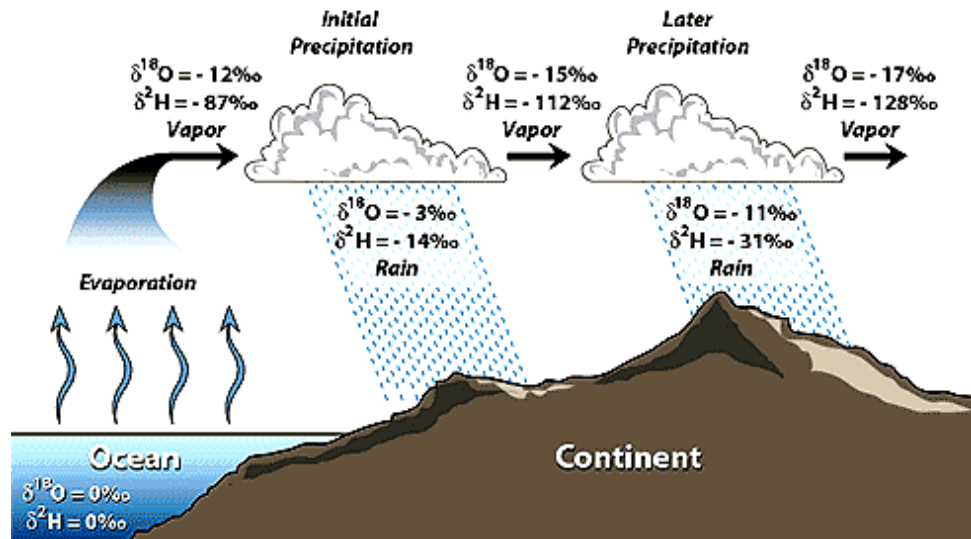


Figure 3: Rainout effect on $\delta^2\text{H}$ and $\delta^{18}\text{O}$ values (SAHRA, 2010).

2.) Amount effect: This effect mainly occurs at oceanic islands and at coastal areas of the tropical regions where seasonal variations of temperature are low. It can be understood as a consequence of the extent of the rainout process of deep convective clouds producing rainfall in these regions and causing isotope depletion (more negative δ values) (Araguas-Araguas et al., 2000). It is observed that the water, collected during smaller rainstorms, is generally more enriched than the water collected during larger rainstorms (Kendall and McDonnell, 1998).

3.) Seasonal effect: Likewise, this effect is caused by the influence of temperature on the isotope fractionation. The extent of seasonal variations in temperature increases with the continentality of the site (Clark and Fritz, 1997). The seasonal change from warm summers to cold winters is reflected in the increasing depletion of the δ values. Figure 4 shows the seasonal variation in $\delta^{18}\text{O}$ values at different stations in North America. Those with the greatest seasonal temperature differences show the greatest seasonal variation in $\delta^{18}\text{O}$ values, for example Gimli and Resolute.

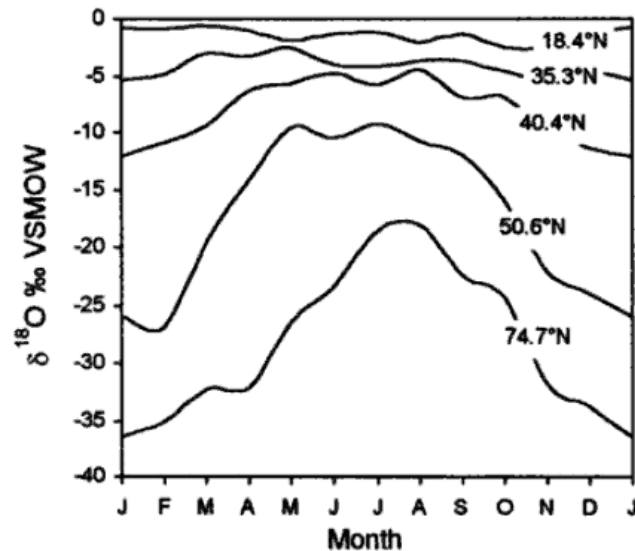


Figure 4: Seasonal variation in $\delta^{18}\text{O}$ in precipitation at stations from low to high latitude in North America. The data are for monthly averages at: San Juan, Puerto Rico (18.4°N), Cape Hatteras, North Carolina (35.3°N), Coshocton, Ohio (40.4°N), Gimli, Manitoba (50.6°N), and Resolute, Northwest Territories (74.7°N) (Clark and Fritz, 1997).

4.) Latitude/ temperature effect: As described above, temperature has a very strong effect on isotope fractionation. Therefore, the amount of fractionation is high, especially at cold conditions: the higher the latitude the more depleted are the δ values.

5.) Altitude effect: Temperature decreases with altitude. Thus, this is another temperature driven effect. The effect of altitude on the $\delta^{18}\text{O}$ values is shown in Figure 5. The higher the elevation is, the colder are the conditions, and the more negative are the $\delta^{18}\text{O}$ values of precipitation (Clark and Fritz, 1997). The altitude effect has been recognized in almost all the major mountain belts of the world. It is most often expressed as an isotopic lapse rate and given as a per mil change in $\delta^2\text{H}$ or $\delta^{18}\text{O}$ of precipitation per 100 meters of elevation change (Poage and Chamberlain, 2001).

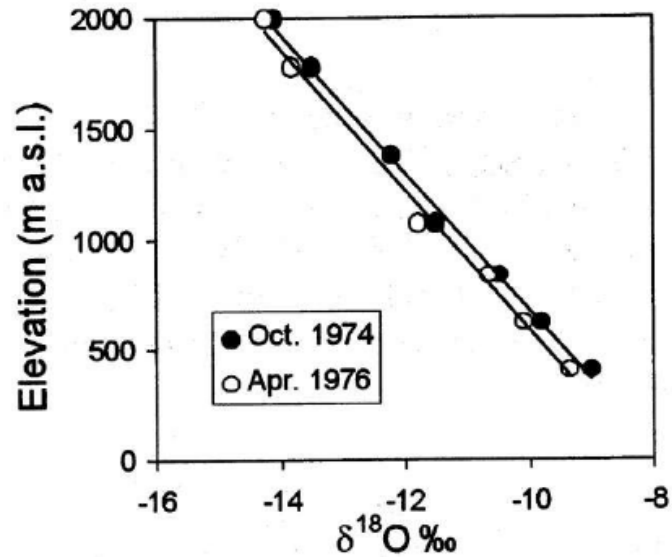


Figure 5: The altitude effect on local rainfall in the Italian Alps (Clark and Fritz, 1997).

1.1.4 Application of stable water isotopes

Stable isotopes of water - as some kind of natural tracers - can assist in the solution of hydro-geochemical and biological problems because of their overall existence. The following section describes examples of application of stable water isotopes: first, in plant ecology and second, in soil science.

Stable isotope analyses of both hydrogen and oxygen improve the understanding of water source acquisition by plants and provide insights across a range of spatial scales from the cell to the plant community, ecosystem, or region, and over temporal scales, since the “pools” of water used by plants can simply be distinguished (Dawson et al., 2002). It is easy to apply $\delta^2\text{H}$ and $\delta^{18}\text{O}$ data to water acquisition studies because there is no change in the isotopic composition of water during uptake and transport in roots and stems by terrestrial plants (Figure 6).

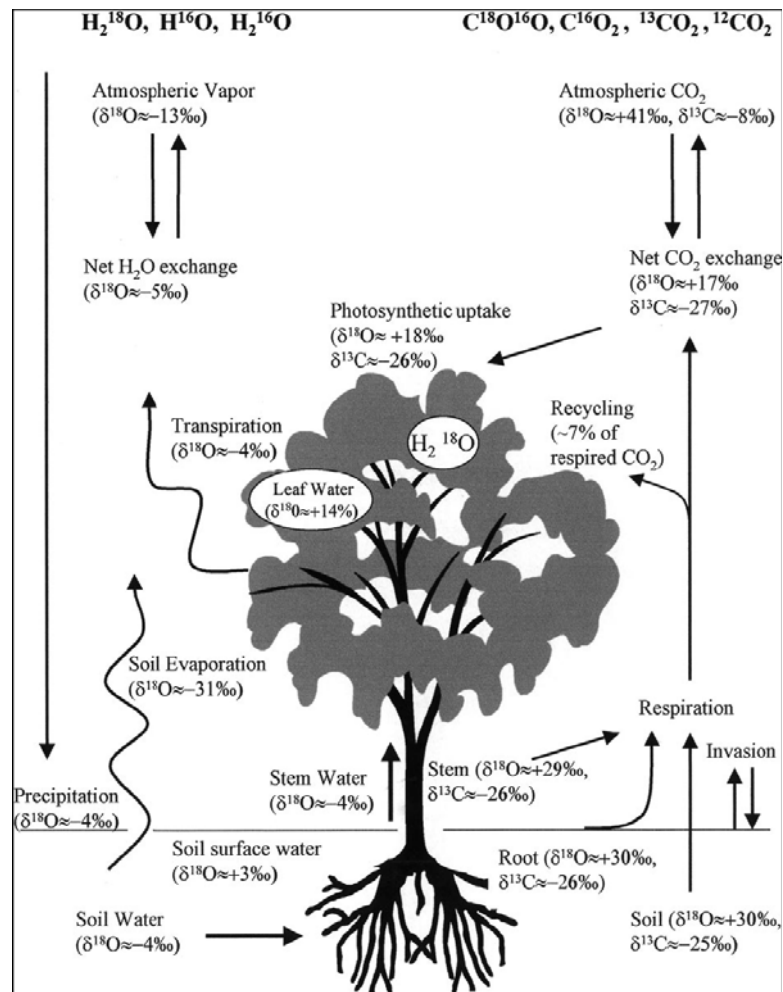


Figure 6: Isotopic composition of C and O pools in the carbon and water cycles. The values are rough approximations and can vary greatly with geographical location and environmental conditions (Yakir, 2000).

There is, however, an evaporative enrichment in the leaves, which varies daily and depends on humidity gradients, transpiration rate, and the isotopic composition of atmospheric water (Wang and Yakir, 2000). If samples of the different water sources of plants – soil water, xylem sap, leaf -, and stem water – are extracted, for example, by cryogenic vacuum extraction and analysed for their water isotope signature, it is possible to assess the origin of water used by plants (groundwater, deep and shallow soil water or surface water) in comparing their signature. Beyond that, water isotope analyses can be a tool for determining intra- and interspecific resource competition and community water-use patterns or the zones of root activity in soils (University of Utah, Isotope course, 2009). Additionally, the difference in water uptake between summer and winter can be identified. For instance, White et al. (1985) show that water use by eastern white pine (*Pinus strobus*) switch between deep and surface soil layers depending on the appearance of precipitation events (Figure 7). Right after a rain event, the

white pine trees utilise water from the surface layers. This soil surface water has an isotope signature similar to that of the recent precipitation event.

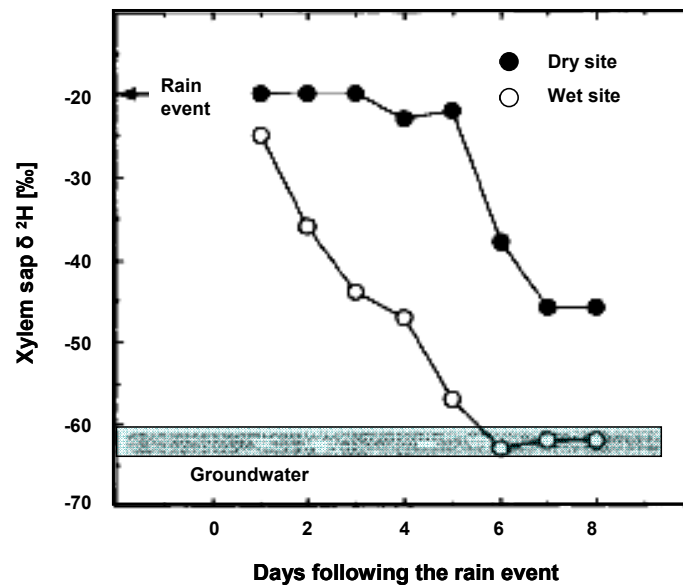


Figure 7: Time course of the hydrogen isotope ratio of xylem sap in eastern white pine (*Pinus strobus*) following a summer rain event. Trees at the wet site had access to a secondary groundwater source, whereas trees on the dry site did not have access to the groundwater (White et al., 1985).

When the surface soil layer dries out (after 3 days at the dry site), the $\delta^{2}\text{H}$ values of stem xylem sap decrease rapidly, indicating a switch from surface soil water to deeper soil layers. The trees at the wet site, which have access to the groundwater, strongly depend on water and, therefore, they switch to the deep water layer more rapidly than the trees on the dry site, indicated by the sharp decrease of their xylem sap $\delta^{2}\text{H}$ values. These data show the capacity of heartwood to change their water use pattern during periods when no rain occurs (no surface water source) or during periods of water deficit. Thus, stable water isotopes provide insights into the water movement within these plants (Ehleringer and Dawson, 1992).

In soil science, the current objectives are isotope soil profiles. They can provide information on water fluxes through the soil, interactions between surface- and groundwater, capillary rise of groundwater, or on water losses due to soil water evaporation. Generally, in saturated soils the highest δ values are observed at the soil surface (Figure 8). There, evaporation leads to isotope fractionation. Further, a highly enriched “evaporation front” usually develops at 0.1 – 0.5 meter below the soil surface. However, below that front, the isotope enrichment decreases exponentially with depth to the value of the source water in the system (Wang and Yakir, 2000).

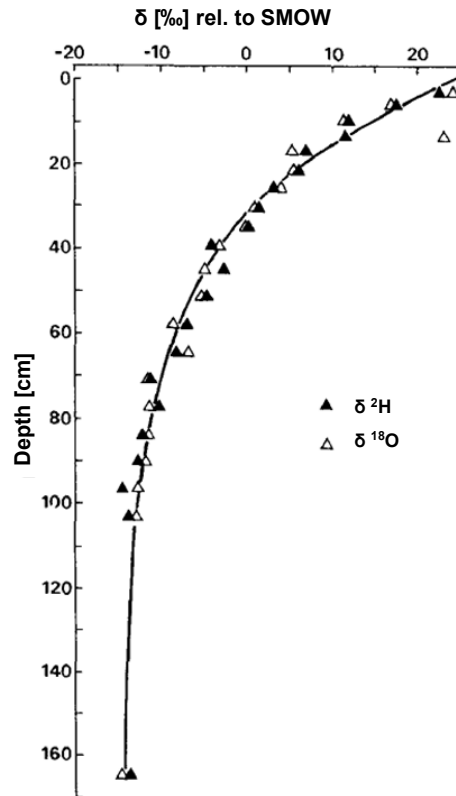


Figure 8: Depth/ δ value relationship for steady-state evaporation from a saturated sand column. The $\delta^{18}\text{O}$ profile is scaled onto the same curve as the $\delta^2\text{H}$ profile (Barnes and Allison., 1988).

For unsaturated soils the isotope depth profile does not have such a uniform appearance, but it can also provide information of the history of the water body in the soil. It should be mentioned that these isotope soil profiles as well as the isotope signature of plant material are only a snapshot and, therefore, vary greatly (Ghosh and Brand, 2003).

1.2 Hydrogen and oxygen isotope analysis

In general, two main types of isotope ratio analysing methods exist: Mass spectrometry and diode laser absorption spectroscopy, both described in the following.

1.2.1 Mass spectrometry

Mass spectrometric methods are very effective means of measuring isotope abundances. A mass spectrometer separates charged atoms and molecules on the basis of their masses and motions in magnetic and/or electrical fields. Since there are abundant types of mass spectrometers, only the principles will be described briefly in this thesis. Generally, a mass spectrometer consists of four different central constituent parts: the inlet system (injecting the sample and the reference standard into the system), the ion source (converting molecules into ions), the mass analyser (recording the masses of the ions), and the ion detector (detecting the mass-to-charge-ratio) (Hoefs, 2009). In any case, the sample is ionized by electrons in the ion source; ions are accelerated down a flight tube between the poles of a magnet, and then are deflected in proportion to their mass-to-charge-ratio (Boutton and Yamasaki, 1996).

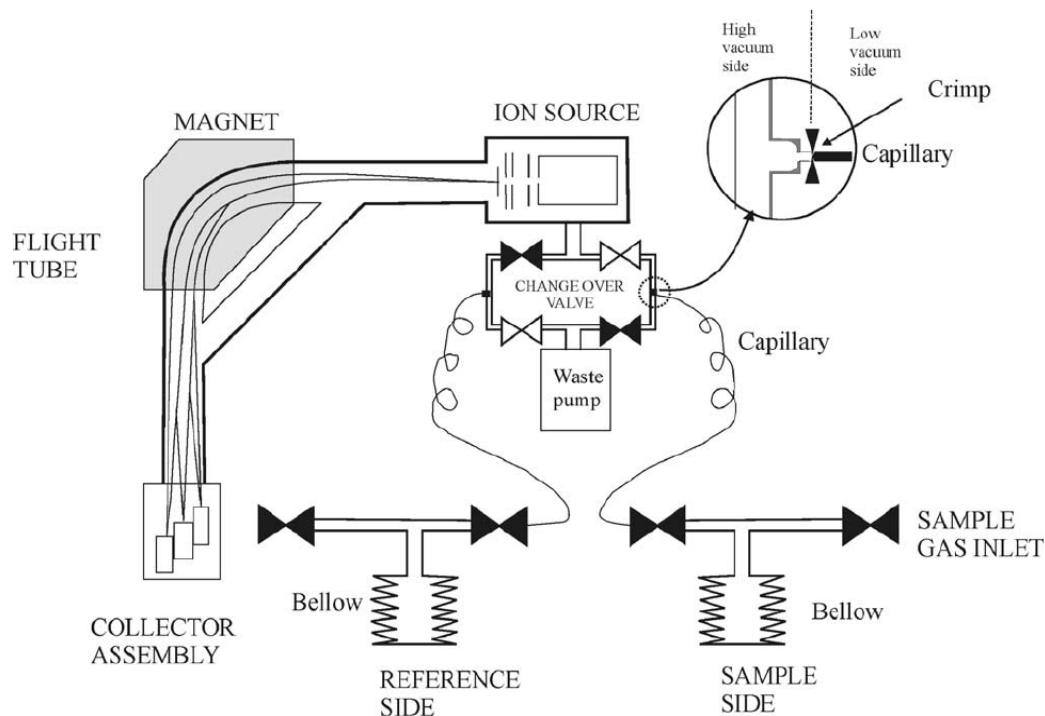


Figure 9: Essential components of a gas isotope mass spectrometer with Dual Inlet system for reference and sample material. In the upper right a close-up view of the capillary with crimp connection is shown (Ghosh and Brand, 2003).

Most conventional mass spectrometers are dual inlet machines that have a sample and a standard inlet. In such instruments, the ratios of the isotopes of interest in the sample are measured compared to the same ratios in a gaseous standard that is analysed simultaneously (Figure 9).

Another type of stable isotope mass spectrometer is the so-called continuous flow mass spectrometer, where gas chromatography and mass spectrometry are connected (Figure 10) (Kendall and McDonnell, 1998).

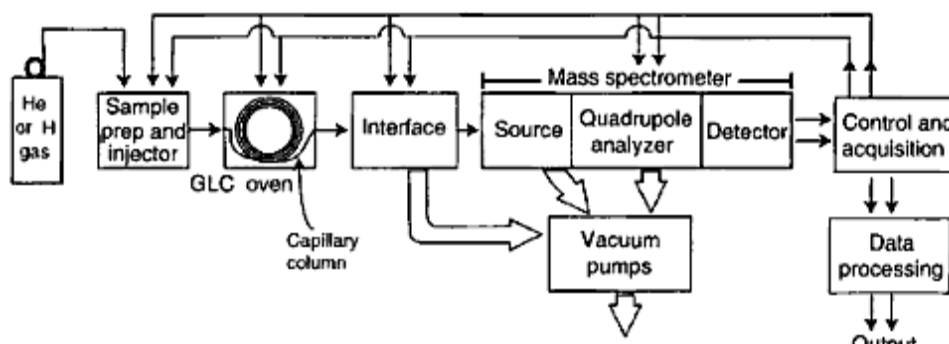


Figure 10: A typical GC/MS system diagram (McMaster, 2008).

The basic parts of a gas chromatographic mass spectrometer (GC/MS) are the inert carrier gas (usually Helium for carrying the injected sample onto and down the capillary column where the separation of the sample occurs and into the interface), the sample injector (injecting the sample into the system), the GC-oven (separating the sample into its compounds between the stationary and the mobile phase according to the polarity to the stationary phase) with its capillary column – the stationary phase –, the interface (as a transfer line between the GC and the MS), and the MS (McMaster, 2008).

1.2.2 Diode laser absorption spectroscopy

Laser-based methods use adjustable diode laser in near- or mid-infrared, to quantify the molecular densities of the isotopes of water in vapour in an optical cell by measuring the transmitted radiation. Infrared spectroscopy, at sufficiently high spectral resolution can, therefore, measure isotope ratios directly in the gas phase, on very small sample sizes (Berman et al., 2009). In absorption spectroscopy, in contrast to mass spectrometry, different isotopic molecular species can be distinguished irrespective of their masses (Kerstel et al., 2002) and, moreover, the ratios of $^1\text{H}/^2\text{H}$ and $^{16}\text{O}/^{18}\text{O}$ can be measured simultaneously (Lis et al., 2008).

In comparison with a conventional isotope mass spectrometer, laser-based technology for the measurements of liquid water isotopes yields comparable or better accuracy. This method is, therefore, fully suitable for high-precision routine isotopic analysis of natural waters (Lis et al., 2008).

A tuneable diode laser produces infrared radiation, which is absorbed by the isotopes in the water sample injected in the system and vaporised in an optical cell under vacuum (Figure 11). The optical cell traps the laser photons so that they make thousands of passes before leaving the optical cell. Therefore, the optical path length may be several thousands of meters using high-reflectivity mirrors and the measured absorption of light, is significantly enhanced (Wang et al., 2009). The optical absorption is measured by a photodetector and converted into the isotopic composition in the water sample by comparing it with a standard water sample of a known isotopic composition.

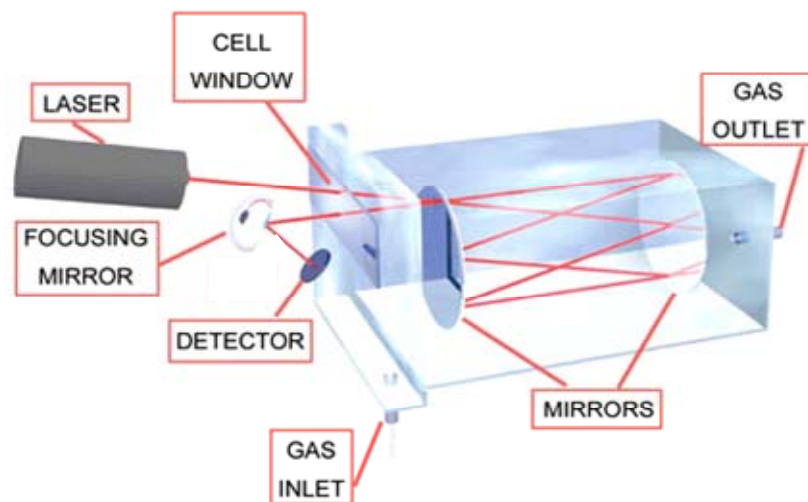


Figure 11: Principle of Tunable Diode Laser Absorption Spectroscopy (Delta F Corporation, Moisture Analyser, 2010).

1.3 Soil and plant water extraction methods for isotopic water analysis

To determine the isotopic signature of environmental water, it is necessary to separate the water from the other components of the sample media (plant material, soil). Therefore, several extraction methods have been developed. Azeotropic distillation, cryogenic vacuum extraction, and centrifugation are the most common ones. However, azeotropic distillation and cryogenic vacuum extraction are the most widely used methods to obtain extracts suitable for isotopic water analysis (Peters and Yakir, 2008). In the following, all these water extraction methods are described.

1.3.1 Azeotropic distillation

Azeotropic distillation uses various toxic substances (toluene, hexane, and kerosene) to remove the water from plant or soil samples (Vendramini and Sternberg, 2007). This procedure is based on the property of some solvents (toluene, hexane, kerosene) to form an azeotropic mixture with the evolving sample water, denoting a boiling point lower than the boiling points of the two components (Sacchi et al., 2001). In the case of a water-toluene mixture, the boiling point is 84.1 [°C], significantly lower than the boiling point of water (100 [°C]) and toluene (110 [°C]). However, at room temperature, the azeotrope floats on top of the water and is not mixable (Revesz and Woods, 1990).

For water extraction, the sample is placed in a modified Soxhlet apparatus (Figure 12), immersed in the selected solvent (for example toluene), and gradually heated. At the boiling point of the azeotrope, the mixture (water and solvent) evaporates, re-condenses in the funnel, forms two phases at room temperature, and then, the evolved sample water can be collected (Ingraham and Shadel, 1992).

For the water extraction from plant material, the sample must be crushed before placing it in the distillation apparatus. Additionally, it is important to add enough solvent so that the sample remains covered throughout the entire distillation process (Revesz and Woods, 1990).

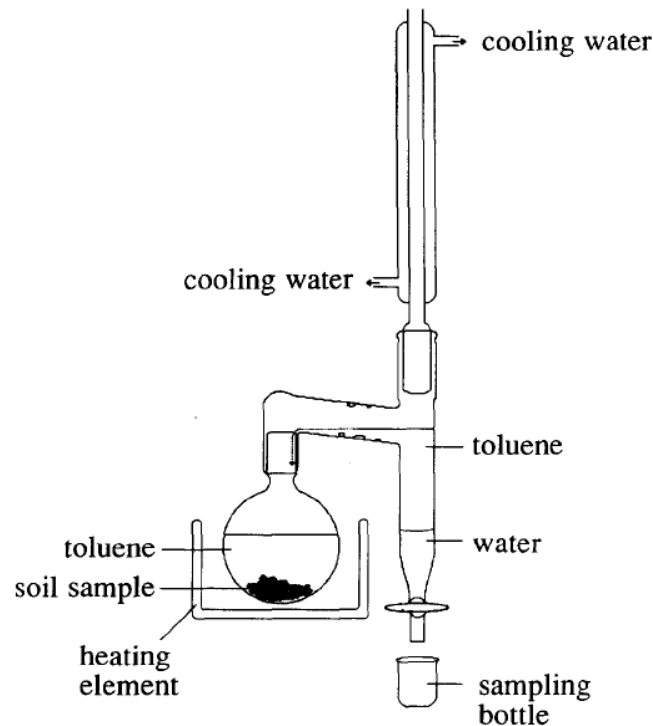


Figure 12: Azeotropic distillation apparatus for soil-water extraction (Revesz and Woods, 1990).

1.3.2 Centrifugation

To apply the centrifugation method for plant and soil water extraction, the sample has to be homogenised (soil) or pulverised (plant material). After that, the sample is placed in a centrifuge extraction tube (Figure 13, A). The included filter adapter composition (Figure 13, B) serves as a physical barrier ensuring the transport and filtration of the extracted water to the bottom section of the centrifuge extraction tube upon centrifugation and an easy collection of the extracted water (Peters and Yakir, 2008).

For the extraction, the centrifuge extraction tube is spun in a centrifuge at a given number of rotations per minute [rpm]. In the case of leaves, Peters and Yakir (2008) centrifuged the samples at 12000 [g] for 10 minutes at 48 [°C] and 10000 [rpm]. During centrifugation, an intense pressure develops, exceeding the capillary tension, holding the water in the sample's pores and causing the water to be extracted.

For a better extraction effort, heavy liquids, immiscible with the water can be used. They percolate through the pores of the sample and push out the solution floating on the top of the sample (Sacchi et al., 2001). The extracted water can then finally be pipetted into vials for isotopic analysis.

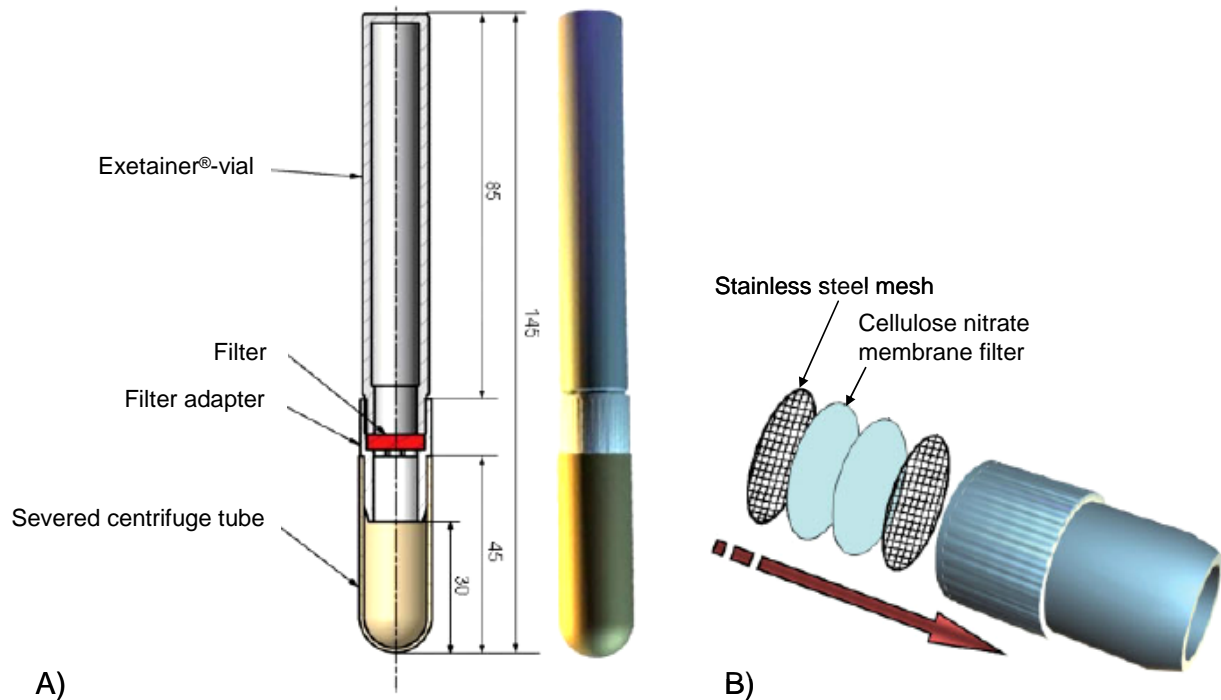


Figure 13: A) Centrifuge extraction tube and B) Filter adapter composition. All measurements are in mm (Peters and Yakir, 2008).

1.3.3 Cryogenic vacuum extraction

With the cryogenic vacuum extraction the plant or soil material is heated in a vessel under vacuum. The sample water is extracted by evaporation and the evolved vapour is frozen in a liquid nitrogen (cryogenic) cold trap (Ingraham and Shadel, 1992). After defrosting the obtained sample water its isotopic signature can be analysed.

This method provides consistent high precision and accuracy for water distilled from several types of plant tissues and soil. However, it requires a complex vacuum system and the duration of the extraction process is much longer than for the azeotropic or centrifugation method (Vendramini and Sternberg, 2007).

There are several different types of cryogenic extraction devices existing for different purposes (soil or plant material – leaf or stem tissue). One of the first published constructions of cryogenic vacuum devices is shown in Figure 14. The device utilised by Dalton (1988) consists of a vacuum pump, a safety trap, a cold finger immersed in a mixture of alcohol and dry ice maintained at a temperature of -64 [°C], and a vacuum flask for the soil. The soil flask is placed in a vessel containing Ethylene and Glycol, which are heated to 104 [°C] for an extraction period of approximately 12 hours. During the distillation process, the total amount of the vaporised soil water is transferred to the cold finger where it condenses. The water is finally collected and analysed for the stable water isotope signature.

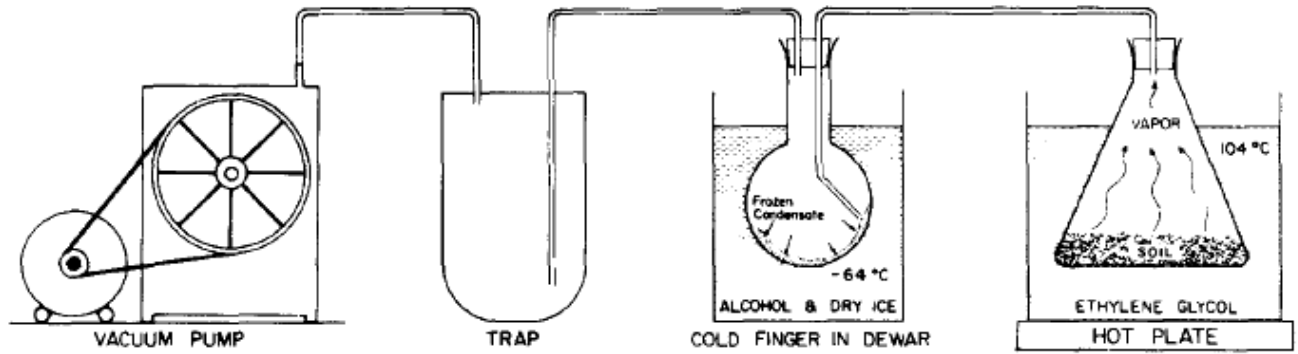


Figure 14: Schematic of equipment used to extract soil water (Dalton, 1988).

This principle was refined and extended for the application of plant water extraction.

West et al. (2006) described a vacuum extraction device for both soil and plant water extraction, which is in common use. It consists of six independent glass units all attached to a 1-inch stainless steel vacuum manifold (Figure 15).

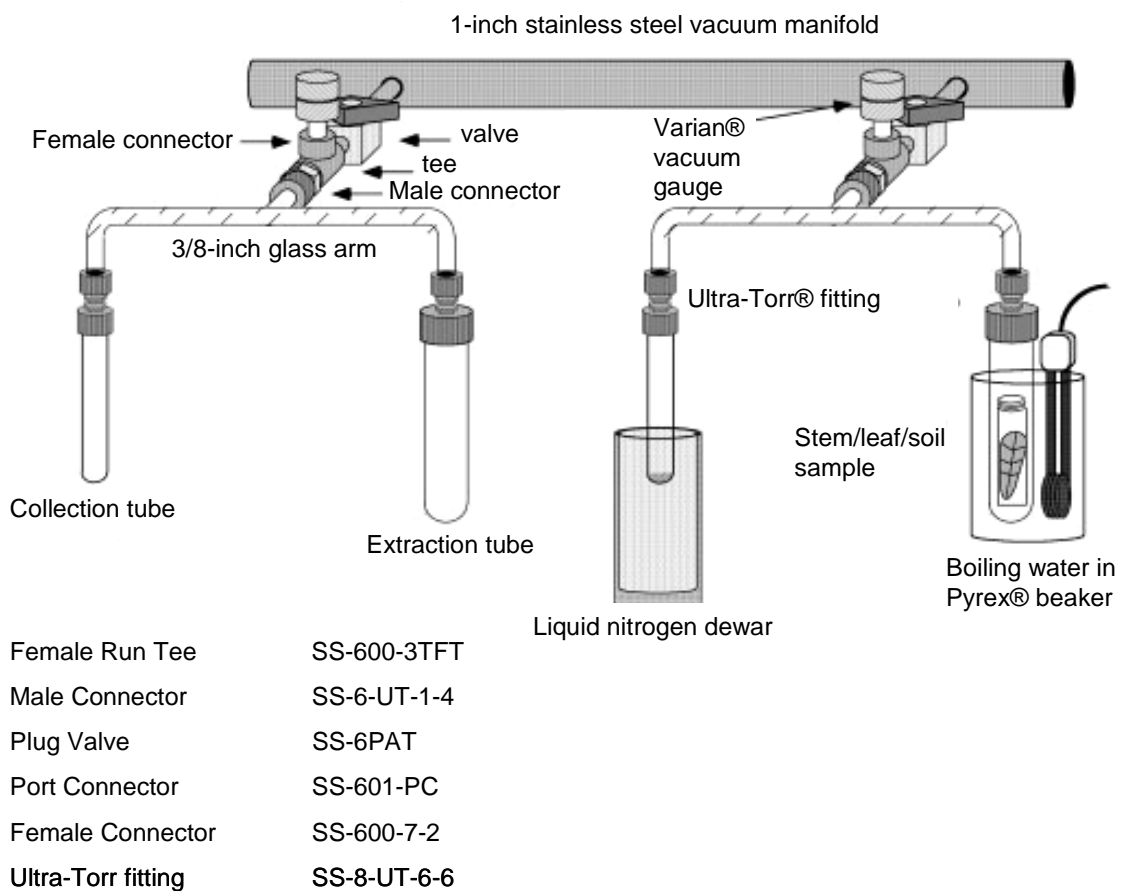


Figure 15: Schematic of a cryogenic extraction line (West et al., 2006).

Each unit consists of 3/8-inch glass arm connected to the manifold via a vacuum gauge (Varian® 801) and can be isolated from the manifold by a NUPRO® plug valve. At each end of the 3/8-inch glass arm, a water collection tube (1/2-inch Pyrex®) and an extraction tube (1-inch Pyrex®) are attached. All connections are made via Ultra-Torr® vacuum fittings or pipe connectors (Swagelok®). The required vacuum is generated by the Edwards® RV5 vacuum pump connected to the vacuum manifold.

For the water extraction, an evacuated unit is isolated from the vacuum manifold while the sample is placed in the extraction tube, which is then reconnected to the unit. For soil samples, glass wool is packed above the sample to prevent the spread of soil particles through the extraction device. Next, the whole unit is pumped down with a pressure of approximately 7.91 [Pa] and the extraction tube is placed in a beaker containing water and a heating element. While the collection tube is placed in a liquid nitrogen dewar to freeze out the evaporating sample water, the water in the beaker is brought to the boiling point, i. e. the sample in the extraction tube is boiled during the whole extraction process.

After the completion of the extraction (for leaves and needles: 20 – 30 minutes, for soils 30 – 40 minutes and for stems 60 - 75 minutes), the boiling water and liquid nitrogen are removed from the collection tube and the extraction tube, respectively. The vacuum pump is shut off and the collection tubes are removed from the system and are defrosted. The extracted water is then pipetted into vials for analysing their isotopic water signature (West et al., 2006).

The United States Environmental Protection Agency (EPA), Integrated Stable Isotope Facility (ISIRF) utilises a water extraction device composed of mainly self-made materials. It consists of ten independent units for soil and plant water extraction (EPA, 2009) (Figure 16).

It is extracted for about 4 hours (for soils and plant material). After three hours of water extraction, an additional vacuum is applied to increase the extraction efficiency. When the water extraction is completed, the water condenser trap is placed into a beaker of room temperature water to defrost the sample.

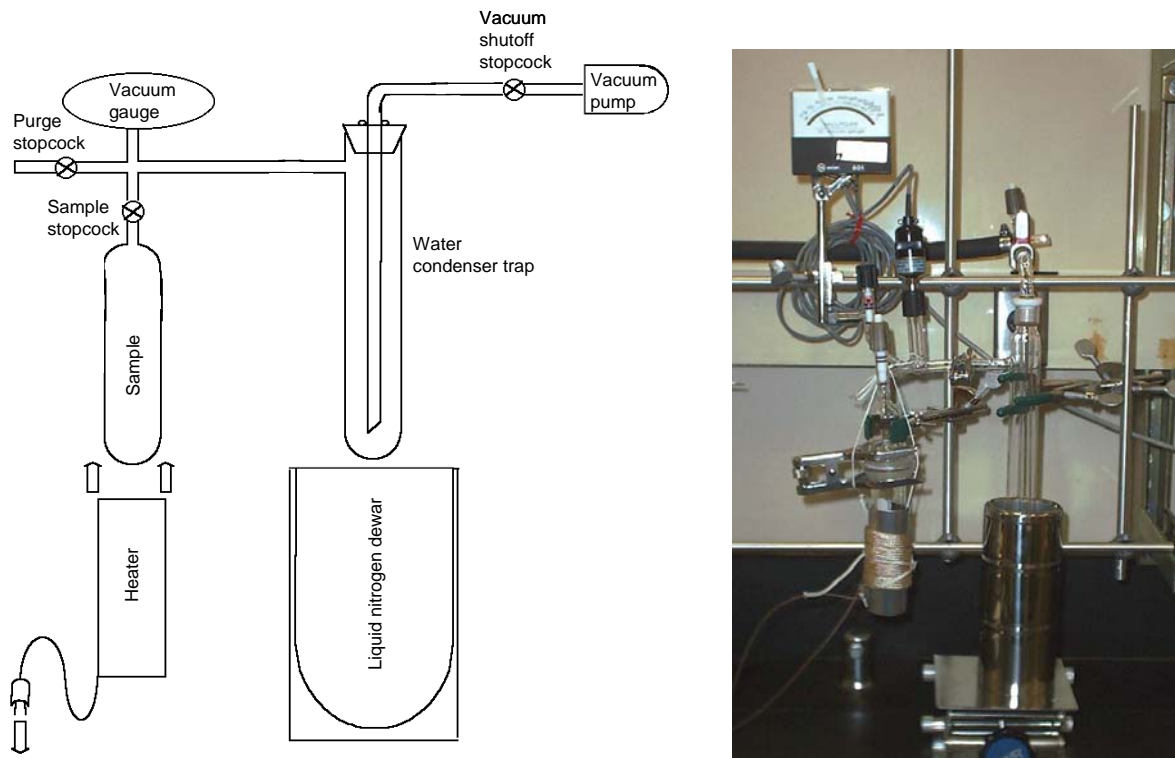


Figure 16: Schematic and photography of the device for extracting water from soils and plants of the ISIRF (EPA, 2009).

At the Paul Scherrer Institute (PSI, Villigen, CH), the cryogenic vacuum distillation apparatus shown in Figure 17 is used to extract water from both soil and plant material (stem, twig, leaf). The extraction device consists of twenty units, whereas five units are joined together via a kind of fork and connected to a stainless steel vacuum manifold (1 meter length) via flexible wave hoses. Each of the five units can be used independently. However, not only one sample can be extracted separately. The extraction and collection tubes (U-tubes) are handmade glassware. All connections are made via Ultra-Torr fittings (Swagelok®). The vacuum stopcocks for applying or shutting off the vacuum are Swagelok® diaphragm valves.

During extraction (2 hours for soil samples, 3 hours for twig samples), the extraction tubes are immersed in a warm water bath at 80 [°C], the collection tubes in a liquid nitrogen dewar, and a pressure of maximum 5 [Pa] is applied.

At the end of every extraction, the U-tubes are removed from the vacuum line and the melted ice is transferred into glass vials for isotopic water analysis (Otieno et al., 2006).



Figure 17: Photography of cryogenic vacuum extraction device for soil and plant material of the PSI (Own source).

Other vacuum extraction procedures are described by Vendramini and Sternberg (2007). They distinguish between the online (similar to the method described by West et al., 2006) and the batch extraction procedure for stem tissue.

In the online method, the distillation arms are evacuated to 1.33 [Pa]. Vendramini and Sternberg (2007) have extracted the samples for a period of 6 hours (for soils) and the distillation arms of the sample vessels have been heated with a torch to prevent the condensation of water on the inner surface of the glass arms.

For the batch method to extract stem water (Vendramini and Sternberg, 2007), the apparatus shown in Figure 18 is used. However, this method is only applied to stem material. Nevertheless, due to its similar extraction principle it is presented in this context.

The apparatus consists of a cooling and a heating pair of anodised aluminum blocks (VWR, modular heating blocks for standard test tubes). The bottom cooling pair of blocks is immersed in a tray containing anti-freeze liquid (VWR, bath fluid Dynalene HC 50) and cooled with an immersion chiller (VWR, immersion chiller, model 1107). The heating element is heated by a dry block heater unit (VWR, analog dry block heater), which is set on a temperature of 100 [°C] during extraction.

For the extraction process, the sample tubes (Pyrex®, glass ware) have to be prepared by sealing one end and fire polishing the other end. The stem samples are then inserted into the tubes and fixed with a wire mesh. After that, the sample tubes are fitted into a vacuum line (via Swagelok®, Ultra-Torr), frozen in liquid nitrogen and further evacuated. Before placing the tubes in the heating-cooling-system, they have to be flame-sealed.

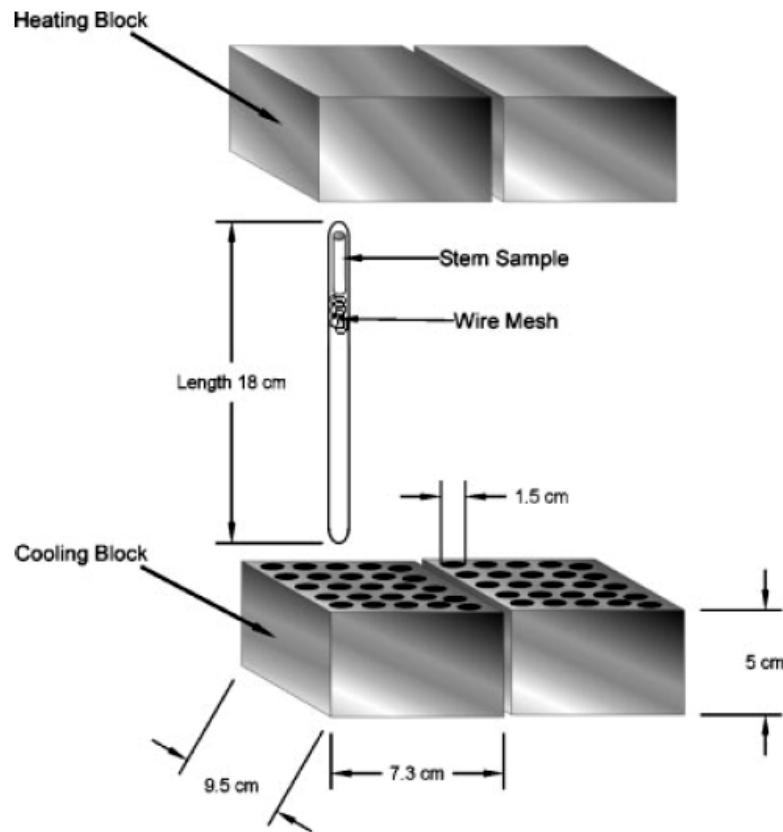


Figure 18: Apparatus for the batch distillation of plant stem-water samples (Vendramini and Sternberg, 2007).

The extraction procedure is started by heating the sample tubes for 1 hour without cooling them. Next, the cooling block is brought to about -25 [°C] for 4 hours. For a period of 8 hours no cooling takes place. The extraction process is finished after another period of 4 hours of cooling the tubes. The 8 hours interruption of the cooling period should increase the distillation efficiency by melting any frozen water blocking the path to the cooling block.

In essence, depending on the usage of the individual water extraction device and for different applications, the cryogenic water extraction distinguishes in the extraction period, the heating temperature, and the used vacuum. Sala et al. (2000) extract for 45 to 90 minutes (for soil, leaf or stem samples) applying an extraction device similar to the one described by West et al. (2006), which is the most common one. For soil water extraction, Ingraham and Shadel (1992) apply a vacuum of 0.13 [Pa] and extract for 7 hours. Whereas, Peters and Yakir (2008) pressure leaf samples at 0.13 [Pa] and heat them at 60 [°C] for 4 hours and Dawson and Ehleringer (1993) extract water from stem samples for 1 hour.

However, a general condition that has to be kept is that the water extraction must proceed to a completion to obtain an unfractionated water sample and, therefore, an overall declaration of

the extraction period, the used pressure, and the heating temperature for all the different existing extraction devices does not make sense.

The cryogenic vacuum extraction device described in this thesis adopts some components of the device from West et al. (2006), some from the device utilised at the PSI (Villigen, CH), but also covers new ideas, such as the high-purity nitrogen aeration after the extraction procedure, instead of aerating the vacuum system after the water extraction process with normal atmospheric air.

2. Materials and Methods

A method to extract water from soil and plant material should be established at the ILR. For the selection of a suitable water extraction method, the following aims were considered:

- to set up a water extraction method for both – plant and soil material –, which is already widely used and approved
- to select a method, which does not use toxic substances for the water extraction, such as the toxic azeotropic distillation
- to choose a method, which does not require a centrifuge
- to construct a mobile device, which can be lend on demand to other research institutes.

For these reasons, the azeotropic distillation method, which uses various toxic chemicals to remove the water from soil or plant material as well as the centrifugation method, where a centrifuge is needed, since it is not available at the ILR, were generally excluded. Thus, the cryogenic vacuum extraction method was particularly suitable.

Subsequently, some general requirements for the new cryogenic vacuum extraction device were formulated. Furthermore, the existing cryogenic extraction devices were studied to decide, which devices to adopt, which materials to chose, and which components to improve.

The following section describes the selection of the used materials and the technical construction of a new cryogenic vacuum extraction device at the ILR.

2.1 Material selection and technical description

The following requirements should be fulfilled regarding a proper selection of materials for the construction of a new cryogenic vacuum extraction device at the ILR:

- an entire vacuum-tight system, guarantying a complete water extraction process with no changes in the isotopic composition of the samples
- user-friendly and easy to handle materials
- extendable modularity with several extraction units
- independently working extraction units with the possibility to extract only one sample
- easy substitutionality of defective material
- utilisation of standard material (off the shelf)
- stainless steel as main material instead of glass due to the risk of breakage

- opportunity to observe the extraction process
- possibility to perform high-purity nitrogen aeration (instead of the aeration with atmospheric air) after each water extraction process and independent for each extraction unit.

Studying the existing cryogenic vacuum extraction devices, the apparatus used by the ISIRF (EPA, 2009) was excluded. Its complexity is not very considered. In addition, it is not possible to adopt a system for the high-purity nitrogen aeration to this apparatus without any difficulties. Moreover, this device does not consist of standard materials, which can hinder a substitution of defective material. The batch method applied by Vendramini and Sternberg (2007) is only suitable for the extraction of stem water and, therefore, excluded, too.

The principle of the method used at the PSI (Villigen, CH) is very similar to that used by West et al. (2006). These two devices mainly utilise stainless steel material for the vacuum system and handmade glassware for the extraction and collection tubes for a visual observation of the water extraction procedure. Additionally, the devices consist of independently working extraction units, which are composed of vacuum-tight standard materials (Swagelok® fittings). This fact guarantees substitutionality of defective material. Furthermore, the size of these devices is ideal to place them on a laboratory-trolley, which makes them mobile. Ultimately, the opportunity to perform high-purity nitrogen aeration after every extraction process – independent for every extraction unit – to create a protective layer of nitrogen gas over the defrosting extraction water is fulfilled with this method. This nitrogen layer should prevent a mixture of atmospheric water vapour with the extracted sample water during the aeration of the vacuum system and, additionally, avoid the evaporation during the defrosting of the extracted water, which would lead to a modified isotopic composition of the extracted sample water.

Hence, the cryogenic vacuum extraction device constructed at the ILR –, described in detail in the following section, – is mainly based on the principle used at the PSI and by West et al. (2006).

Generally, the cryogenic vacuum extraction device of the ILR, placed on a mobile laboratory-trolley, consists of stainless steel materials, mainly Swagelok® fittings and VACOM® components, to generate a vacuum-tight system. It can be subdivided in the **vacuum distribution system** with its six **independent extraction units**, and the **extraction-collection units** for the extraction of the samples and the extracted sample waters (Figure 19).

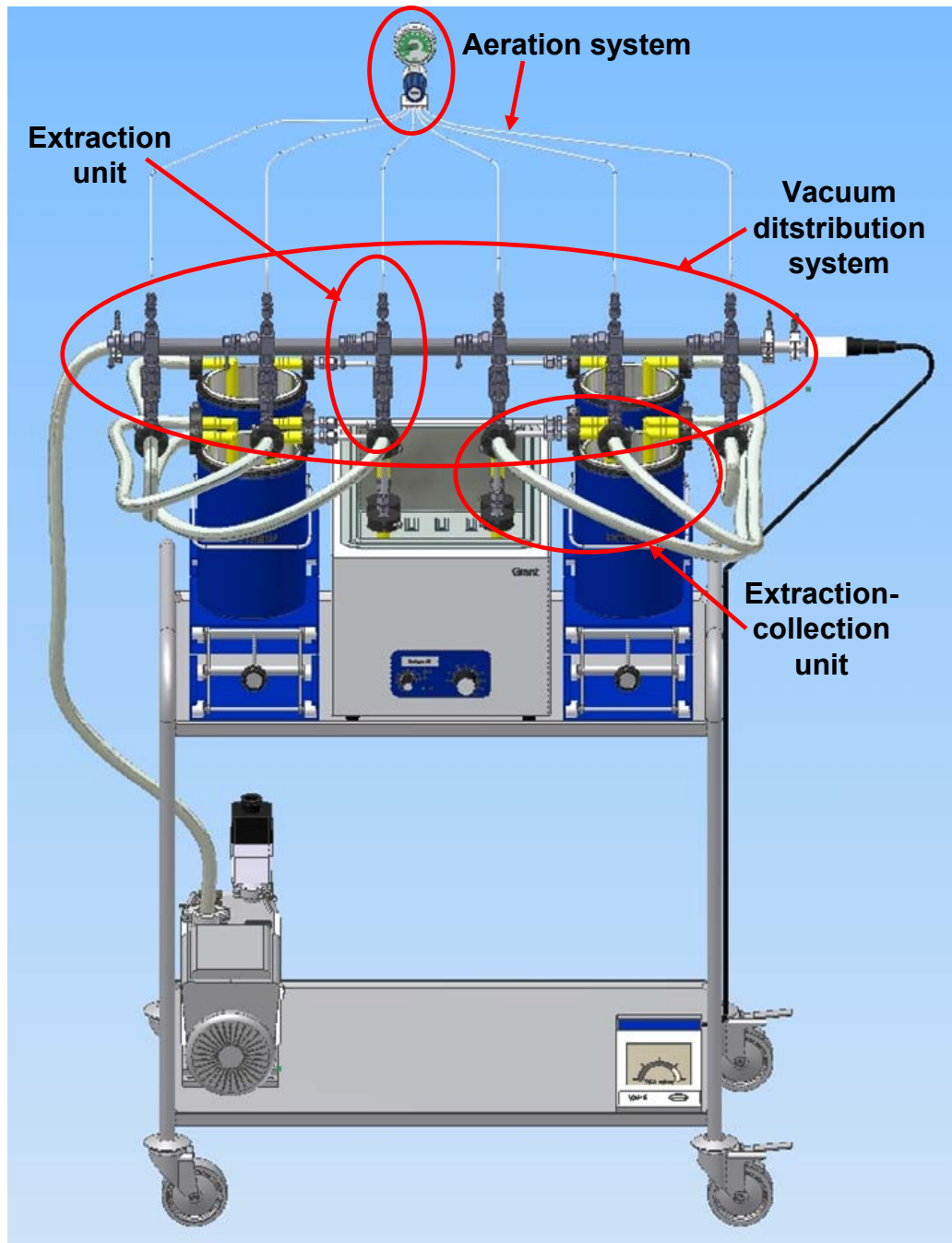


Figure 19: Schematic of the whole vacuum extraction device at the ILR (Own source).

For a detailed visualisation, true to scale technical drawings of the vacuum distribution system and of the whole apparatus are provided as posters (A1 format) at the back of this thesis. The technical drawings and schematics were performed using Autodesk® Inventor® (Autodesk GmbH, Munich, DE). Appendix 1 contains a detailed list of the selected materials including article description with measurements, ordering number, producer's, and distributor-'s' addresses.

The vacuum distribution system

In general, the vacuum distribution of the ILR's device consists of six independent short stainless steel connections (length 10 mm) welded with a seamless stainless steel titanium alloyed tubing (Swagelok®) (Figure 20), similar to the vacuum manifold designed by West et al. (2006). The vacuum is generated by a two stage rotary vane pump (Edwards®, RV5), as by West et al. (2006), which is connected to the stainless steel tubing (length 1000 mm) via a bored flange (DN25), a clamp ring, and a flexible hose (all components from VACOM®) (Figure 19). In order to provide stable vacuum conditions during the whole extraction procedure, the vacuum is observed by a PIRANI® vacuum gauge (VAP 5-set: sensor plus measuring cable), connected to the vacuum manifold via a bored flange, a tubulated reducing adapter (DN25 to DN16), and a clamp ring (Figure 19).

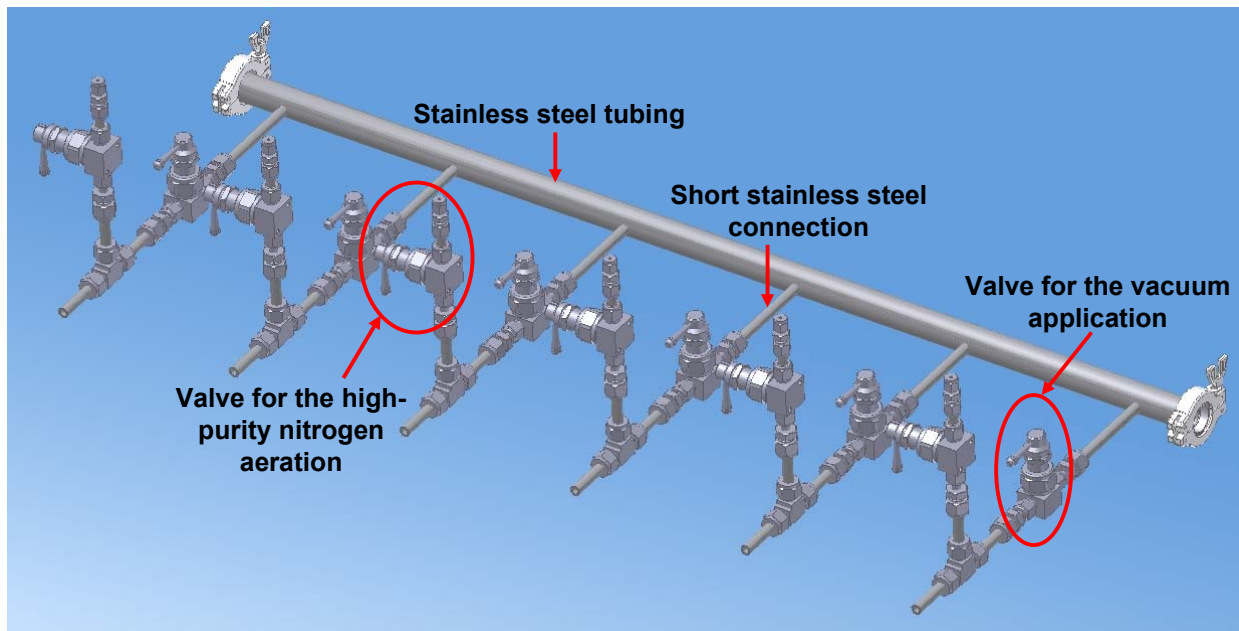


Figure 20: Schematic of the whole vacuum distribution system (Own source).

The extraction units

The six independent extraction units are composed of different types of Swagelok® fittings (Figure 21).



Figure 21: Photography and schematic of one extraction unit (Own source).

The vacuum can be applied or shut off via Swagelok® diaphragm valves (also used at the PSI), which are attached to the welded connection via a reducing tube fitting (10 mm outer diameter to 8 mm).

To construct high-purity nitrogen aeration, additional diaphragm valves are necessary, which are joined via Teflon hoses (3 mm outer diameter) to a nitrogen gas source. These connections are again generated by Swagelok® reducing tube fittings (10 mm outer diameter to 8 mm) attached to union tee fittings over short connection tubes (length 50 mm, 10 mm outer diameter). On the head of the union tee fittings, the additional diaphragm valves are placed via short connection tubes and reducing tube fittings (10 mm outer diameter to 8 mm). The attachments to the Teflon hoses (H. Riesbeck®) are generated by reducing tube fittings: 8 mm to 6 mm (outer diameter) and 6 mm to 3 mm (outer diameter).

To apply the vacuum to the extraction tubes, KF Swagelok-adapters (Vacom®) including DN16 flanges are connected on their one side to the union tee fittings via short connection tubes and on their other side to one end of flexible hoses including DN16 flanges at each end, too. All used flanges are fixed by centering- and clamp rings. The other ends of the flexible hoses are attached via flange-centering-clamp-ring connections to the U-tubes, which collect the extracted water. The water extraction device from the PSI also utilises flexible hoses and

flanges to connect the fiver unit of extraction – a kind of fork – and connection tubes to the vacuum manifold.

The extraction-collection units

The extraction-collection units of the water extraction device consist of glass flanges (Rettberg®, DN16) formed to round-bottom test tubes (extraction tubes) and to U-tubes (collection tubes) (Figure 22, left). This idea is adapted from the PSI's apparatus.

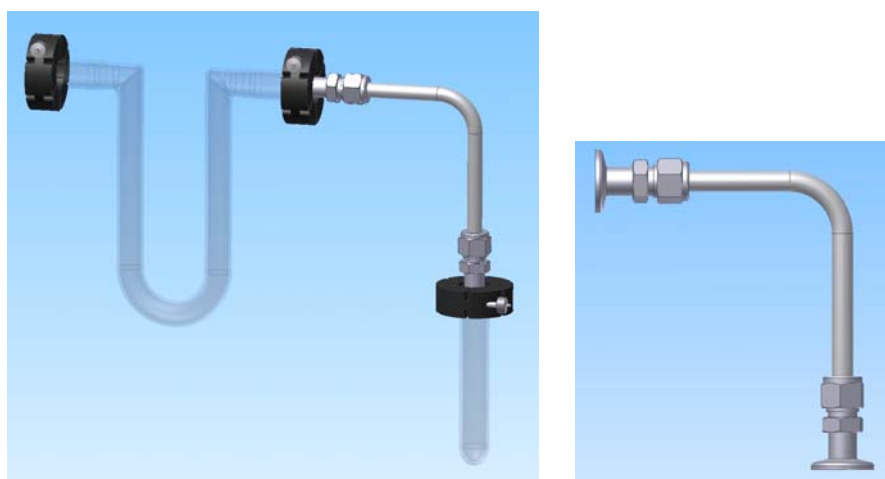


Figure 22: Schematic of an extraction-collection unit and its angular connection tube (Own source).

The extraction and collection tubes are joined together via stainless steel 90° angular connection tubes (10 mm outer diameter, tube length short side: 80 mm, tube length long side: 100 mm) attached to KF Swagelok-adapters (DN16 flanges at each end) (Figure 22, right). The glass flanges of the extraction and the collection tubes can easily be fixed to the angular connection tubes by centering rings and KF clamping chains (Rettberg®, DN16).

During the extraction process, the U-tubes are immersed in liquid nitrogen dewars (VWR®, portable dewar, type 27, version B) and the extraction tubes are boiled in a temperature regulated water bath (VWR®, water bath, JB aqua 18, standard). For a better handling, the liquid nitrogen dewars are placed on labour lifting plates (Th. Geyer®, lab-jack with adjusting wheel).

Generally, the costs for the whole apparatus are in the range of 10000 €.

Photography of the whole extraction apparatus is shown in Figure 23.



Figure 23: Photography of the ILR's cryogenic vacuum extraction device (Own source).

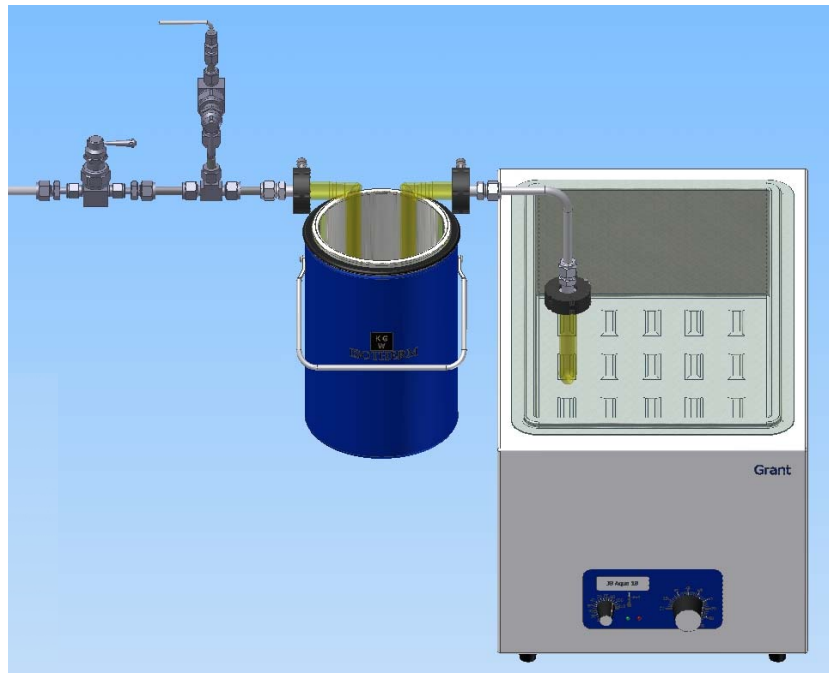
2.2 Procedure of cryogenic vacuum extraction

For stable water isotope analysis of soils or plants, a representative and accurate sampling is important. With regard to the stable water isotopes it is necessary to collect fresh samples, which should directly be kept cold until the water extraction to reduce evaporation, transpiration or biological processes leading to isotope fractionation.

Before starting the water extraction process, water has to be filled in the water bath and heated up to 70 – 80 [°C]. Additionally, the dewars have to be filled with liquid nitrogen. Next, the U-tubes have to be connected via flanges, centering rings, and clamping chains on the one end to their angular connection (Figure 21) and on the other end to the flexible hose of the extraction device. Therefore, the U-tubes should not be immersed in the liquid nitrogen to avoid freezing out of atmospheric water vapour, which changes the original isotope ratios of the samples. After that, an adequate amount of sample material has to be weighted out and placed into the extraction tubes. To fix the sample material in the extraction tubes and to avoid the spread of the sample material inside the extraction device, a piece of fleece is laid on top of the sample material, likewise, applied at the PSI.

Then, a static vacuum of 0.3 [Pa] has to be generated by the rotary vane vacuum pump and observed via the vacuum gauge. During the vacuum generation, all diaphragm valves have to be closed. In the next step, the extraction tubes are attached to the angular connection tube via flanges, centering rings, and clamping chains, but should not yet be immersed in the water bath to prevent a premature evaporation of water from the samples. Then, the diaphragm valves near the vacuum manifold have to be opened for no more than three seconds to draw out the atmospheric water vapour. Afterwards, the U-tubes are frozen in liquid nitrogen and the extraction tubes are situated in the temperature regulated water bath (Figure 24 A and B). Finally, the diaphragm valves near the vacuum manifold are opened and the water extraction begins.

During the whole extraction process, the extraction tubes - including the sample material - are boiled and, thus, lead to the evaporation of water from the sample material (Figure 24 C). This is subsequently trapped in the frozen U-tubes, situated in liquid nitrogen at a temperature of -196 [°C]. Extraction was conducted for two hours to make sure that all water has been withdrawn.



A)



B)



C)

Figure 24: A) Schematic of one extraction unit with its extraction-collection unit.

B) Close-up photography of the extraction-collection units with their angular connection tubes during water extraction (immersed on the one hand in the water bath and on the other hand in the liquid nitrogen dewar).

C) Close-up photography of the extraction tubes including soil samples fixed with fleece immersed in the water bath during water extraction.

After the extraction, the vacuum pump, gauge, and water bath are shut off, the diaphragm valves are closed, and the trapped water in the U-tubes is purged by high-purity nitrogen gas for no more than six seconds via the diaphragm valves above the union tee fittings. This high-purity nitrogen aeration is performed instead of aeration with atmospheric air due to the fact that the atmospheric water vapour could mix up with the extracted sample water, leading to a modified isotopic composition of the extracted water. Furthermore, the layer of nitrogen pro-

hibits the loss of water vapour during defrosting of the extracted water and, thus, prevents isotope fractionation.

After that, the extraction and U-tubes are removed from the extraction device. Subsequently, the extracted water situated in the U-tubes thawed at room temperature and is finally pipetted from the U-tubes into glass vials (2 ml) for analysing its water isotopic composition. The vials are entirely filled, optionally with insets (300 and 450 μ l) and sealed with Parafilm®.

2.3 Validation experiments

Before the constructed cryogenic vacuum extraction device could be used for common stable water isotope research, it has to be tested concerning its proper functioning.

All validation tests were conducted with water instead of soil or plant material. For instance, if leaves had been used for testing, the leaves should have been collected from the same plant, which would have arose problems concerning the natural variation between the leaves of the same plant in the eventual statistical analysis. Furthermore, the leaves should have been pre-treated before water extraction by cutting them into equal sized pieces for a proper comparability. Thereby, transpiration processes could have occurred, changing the stable water isotopic signature of the leaves and leading to isotope fractionation. However, this circumstance is difficult to quantify but would have to be regarded in the analysis of the data. In contrast to plant material, the handling of water as test material for the cryogenic vacuum extraction device is simpler.

Consequently, for a simple implementation of the experiments and proper comparability of the results three different types of water with a known isotopic composition were chosen as testing material: Water from the Schwingbach (Municipal Hüttenberg, Lahn-Dill-District, Hesse, DE), precipitation from Gießen (City Gießen, District Gießen, Hesse, DE), and Gießen's tap water (City Gießen, District Gießen, Hesse, DE). The precipitation was sampled using a cumulative precipitation gauge. All waters were collected at 28/08/09, filled in plastic bottles, sealed with Parafilm® to minimise the possibility of evaporation and kept cold in a refrigerator until water extraction.

The tests of the cryogenic vacuum extraction device were performed concerning the following questions (Table 3).

Table 3: Investigating issues of the validation experiments.

Test	Question	Approach
1.	Does cryogenic water extraction affect the water isotopic composition of the extracted water?	Comparison of the isotopic signature of Gießens's tap water before and after water extraction.
2.	Does the high-purity nitrogen aeration after water extraction affect the water isotopic composition of the extracted water?	2.1 Comparison of the extracted water isotopic signature of Gießen's tap water with and without high-purity aeration after extraction procedure. 2.2 Comparison of the isotopic signature of Schwingbach water before and after water extraction with high-purity nitrogen aeration.
3.	Does cross-contamination among the extraction units appear during water extraction, which leads to a modified water isotopic composition of the extracted water?	Comparison of the extracted water isotopic signature of precipitation from Gießen and Schwingbach water during the same extraction procedure.

Before starting the extraction five original samples from each type of water (Schwingbach water, precipitation from Gießen, and Gießen's tap water) were filled into vials (2 ml) and sealed with Parafilm® to compare them with the isotopic signature of the water after extraction.

For all validation tests each extraction tube was filled 2/3 with testing water and the water extraction procedure described above (Chapter 2.2) was performed. Likewise, fleece was put above the water situated in the extraction tubes, the static vacuum of 0.3 [Pa], as well as a steady temperature of the water bath of 70 [°C] during the whole extraction were applied.

The extraction was finished when all test water situated in the extraction tubes, passed over into the collection tubes, approximately in a time period of three minutes. After the extraction, the trapped water in the collection tubes (U-tubes) was defrosted. From each collection tube

two vials (2 ml) were entirely filled with the extracted water and sealed with Parafilm® for the water isotopic analysis via Los Gatos Research DLT-100- Liquid Water Isotope Analyser (LGR DLT-100) (Los Gatos Research Inc., 67 East Evelyn Avenue, Suite 3, Mountain View, CA, 94041-1529, US).

For the validation test number 3, precipitation from Gießen and Schwingbach water was each filled into three of the six extraction tubes. To test if there was an exchange of water among the extraction units during extraction procedure, leading to mixed waters and a modified water isotopic signature, the extraction tubes of precipitation from Gießen were fixed at the device beside the extraction tubes with the Schwingbach water. After the water isotopic analysis via LGR DLT-100, the statistical analysis of data was performed using PASW Statistics (Version 18.0; SPSS Inc. Chicago, IL, US).

2.4 Analytic measuring method for stable water isotopes

After water extraction, the stable water isotope analysis was conducted using Los Gatos Research DLT-100- Liquid Water Isotope Analyser (Los Gatos Research Inc., 67 East Evelyn Avenue, Suite 3, Mountain View, CA, 94041-1529, US) (Figure 25).



Figure 25: LGR DLT-100-Liquid Water Isotope Analyser (LGR, 2010).

This instrument utilises near infrared absorption spectroscopy to quantify simultaneously the $^2\text{H}/^1\text{H}$ and $^{18}\text{O}/^{16}\text{O}$ ratios of water samples in an optical cell. Laser-based water isotope analysers have several advantages: they do not require extensive consumables or sample conversion. In addition, they require lower power, and the cost per sample is low. However, the sample has to be very clean and should not contain dissolved organic matter or alcohols (Berman et al., 2009).

For the isotope analysis, the glass vials capped with silicone septa, containing 2 ml of the extracted water, are placed into the auto-sampler, which is attached to the LGR DLT-100. To determine the water isotope ratios of an unknown sample, it is necessary to include calibrated stable water isotope standards of different water isotope ratios within each measuring campaign – after every 5th sample the internal standards are measured. For each sample, six sequential 1.2 μL aliquot of a water sample are injected into the optical cell of the LGR DLT-100 via a Hamilton microliter syringe. Then, the first three measurements are discarded. The remaining are averaged and corrected for per mil scale linearity. Before the injected sample enters the optical cell of the LGR DLT-100 it is vaporised. A high vacuum is generated in the optical cell via a vacuum pump. The tunable diode laser of the LGR DLT-100 produces near infrared radiation passing the vaporised water sample in the optical cell. The optical cell, which is equipped with high-reflecting mirrors, traps the laser photons in a way that, on aver-

age, they make thousands of passes through the sample vapour before leaving the cell (Figure 26). As a result, the measured absorption of light by the water isotopes after it passes through the optical cavity is significantly enhanced (Wang et al., 2009). After leaving the optical cell, the remaining laser photons are focused via a lens on a photo-detector, which then detects the optical absorption.

The results of the measurement are matched to the data collection and analysis system, which converts the optical absorption into the isotopic composition in the water sample, by comparing it with the absorption of the internal standard of known isotopic signature (LGR, 2010). After every sample measurement, the water vapour in the optical cell is evacuated (gas outlet).

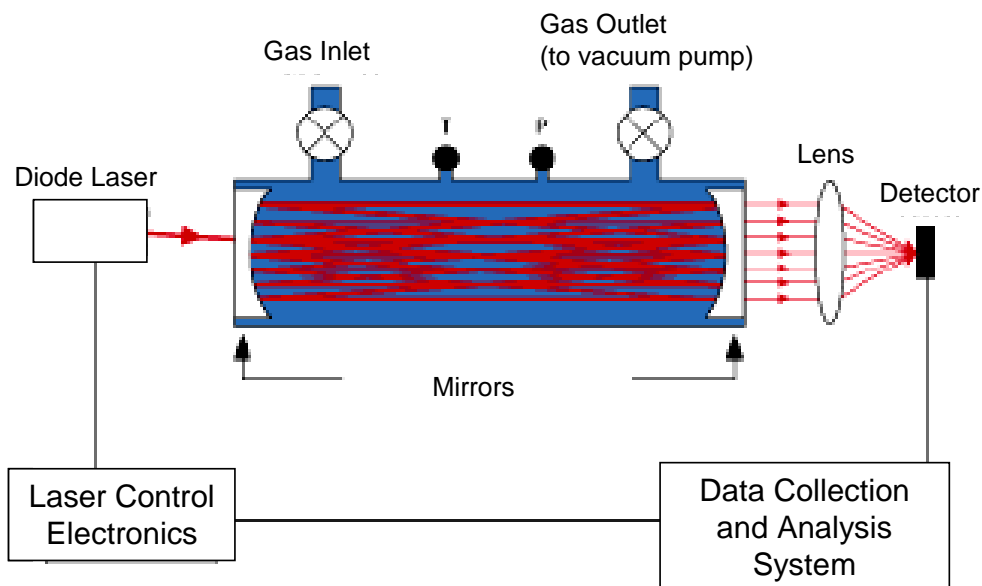


Figure 26: Functional principal of the LGR DLT-100 (LGR, 2010).

All isotope ratios are reported relative to VSMOW. Precision of this method, based on repeated standard measurements, is about 0.2 [‰] for $^{18}\text{O}/^{16}\text{O}$ and 0.6 [‰] for $^2\text{H}/^1\text{H}$ isotopes (LGR, 2010).

3. Results and Discussion

The aim of this thesis was to construct a vacuum-tight, reliable, and user-friendly cryogenic vacuum extraction device with an extendable modularity and several independently working extraction units for the application in stable water isotope research sciences. Furthermore, the new cryogenic vacuum extraction apparatus should be composed of standard materials (off the shelf), should guarantee and easy substitutionality of defective material, and should provide the opportunity to observe the extraction process.

An additional concern was to construct a system for the aeration of the vacuum distribution with high-purity nitrogen gas – after the extraction procedure – instead of aeration with atmospheric air. This system can minimise the possibility of evaporation, leading to fractionated extracted water and, thus, minimise the probability of error. High-purity nitrogen aeration is one option to overcome the problem of evaporative water loss during defrosting of the extracted sample water and the problem of a mixture of the atmospheric water vapour with the extracted sample water, leading to a modified isotopic composition of the extracted water. Nitrogen gas is an inert gas and does not react with the stable isotopes of water and, consequently, does not change the isotopic composition of the extracted water.

To fulfil the aforementioned requirements, existing cryogenic water extraction devices were studied and validated concerning to their type, extent of usage, and their complexity. Finally, the principles of the best existing devices were chosen to build up a cryogenic vacuum extraction device at the ILR.

Due to the positive experiences at the PSI in using Swagelok® components, flanges, and flexible hoses for generating the connections, these materials were chosen for the cryogenic vacuum extraction device at the ILR, too. Using Swagelok® fittings most likely fulfil a vacuum-tight feature. The use of flanges for generating diverse connections additionally guarantees vacuum-tightness. Glassware for a visual observation of the extraction process was chosen for the extraction and collection tubes, same as used for the device from West et al. (2006) and at the PSI. The temperature control during the extraction process is ensured by a temperature-regulated water bath, in which all extraction tubes are immersed during water extraction. Thus, the same temperature is precisely applied to all extracting samples. Furthermore, the vacuum is observed by a vacuum gauge, which guarantees the exact same vacuum conditions during the whole extraction process.

In order to test the functioning of the constructed vacuum extraction device, four validation experiments (1 to 3) were conducted. The results of these experiments are described and discussed below. For a better visualisation of the results, box plots for the $\delta^2\text{H}$ and $\delta^{18}\text{O}$ values were created for each validation experiment. Note that using PASW Statistics no zero scale of the box plots exist. Appendix 2 contains the raw data of the $\delta^2\text{H}$ and $\delta^{18}\text{O}$ values of all validation experiments.

3.1 Impact test on the extracted water isotope signature

Validation experiment 1 was conducted to test whether the cryogenic vacuum extraction procedure affects the isotopic signature of the extracted sample water. Therefore, the five original samples of Gießen's tap water, which did not undergo water extraction process before, and the twelve extracted water samples – respectively the mean of two sub-samples collected from the same U-tube was calculated– were compared. First, the $\delta^2\text{H}$ and $\delta^{18}\text{O}$ values of the stable water isotope analysis were tested separately for normal distribution (Kolmogorov-Smirnov-test, $p = 0.05$). Normal distribution was given for both. Therefore, t-tests could be performed with significance levels α of 5%. Gießen's tap water showed no statistically significant differences in its $\delta^2\text{H}$ and $\delta^{18}\text{O}$ values before and after water extraction (Figure 27 and 28). The medians of the $\delta^2\text{H}$ values before and after extraction are nearly the same – before extraction: -57.86 [‰] and after extraction: -57.61 [‰], likewise the medians of the $\delta^{18}\text{O}$ values before (-8.91 [‰]) and after water extraction (-9.33 [‰]) (Table 4).

Table 4: Descriptive statistics of the $\delta^2\text{H}$ and $\delta^{18}\text{O}$ values of Gießen's tap water before and after water extraction for validation experiment 1.

Measures of dispersion	$\delta^2\text{H}$		$\delta^{18}\text{O}$	
	Before extraction	After extraction	Before extraction	After extraction
Mean	-58.41 [‰]	-57.66 [‰]	-8.99 [‰]	-9.38 [‰]
Median	-57.86 [‰]	-57.61 [‰]	-8.91 [‰]	-9.33 [‰]
Variance	3.64	2.13	0.05	0.09
Standard deviation	1.91	1.46	0.23	0.30
Minimum	-60.63 [‰]	-59.41 [‰]	-9.24 [‰]	-9.98 [‰]
Maximum	-56.59 [‰]	-55.70 [‰]	-8.74 [‰]	-9.05 [‰]

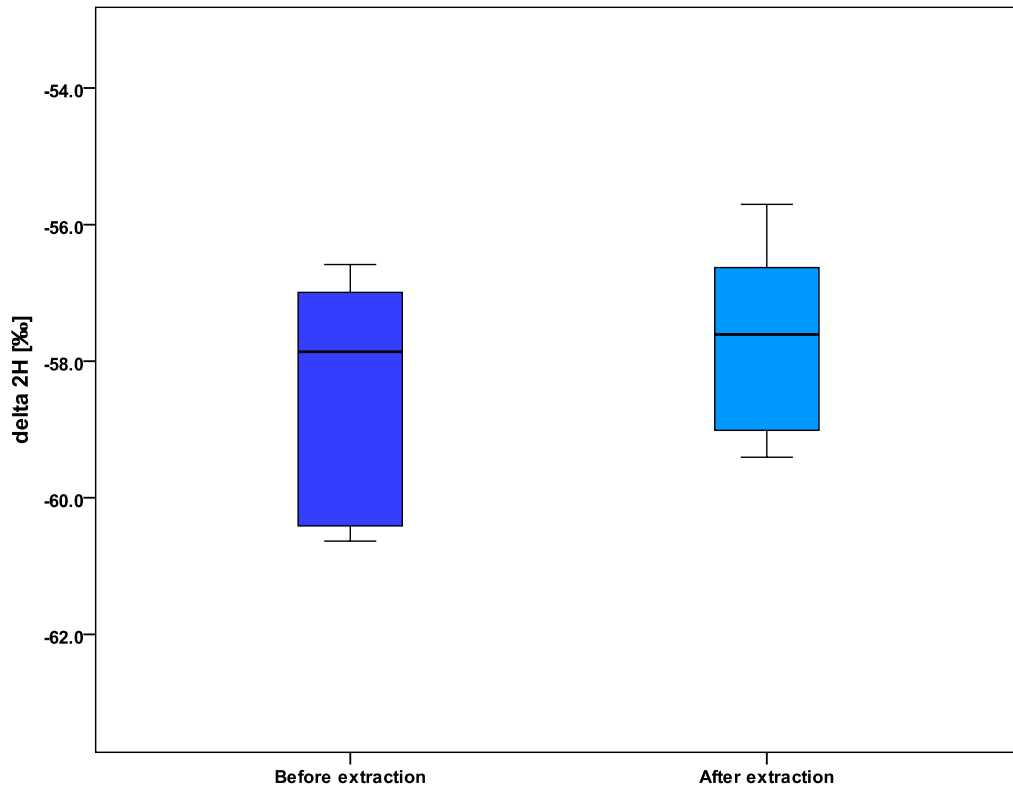


Figure 27: Comparison of the $\delta^2\text{H}$ values of Gießen's tap water before and after water extraction without high-purity nitrogen aeration.

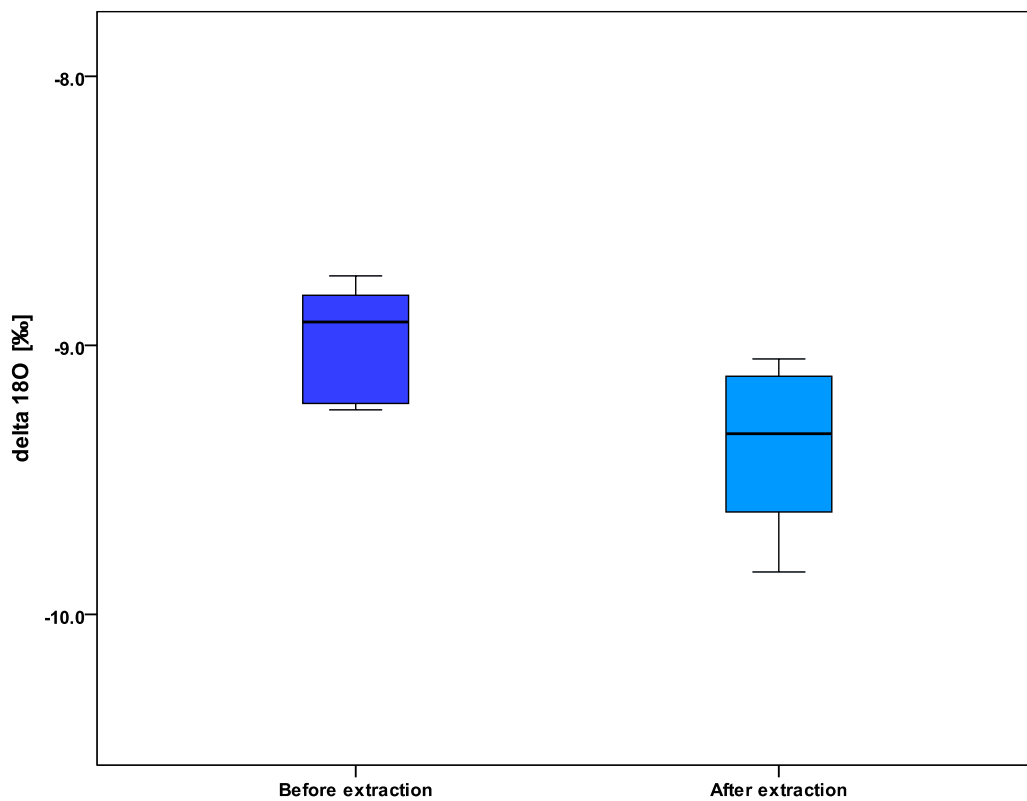


Figure 28: Comparison of the $\delta^{18}\text{O}$ values of Gießen's tap water before and after water extraction without high-purity nitrogen aeration.

The means of these distributions of $\delta^2\text{H}$ are very similar - before extraction: -58.41 [‰] and after extraction: -57.66 [‰]. However, standard deviations and variances for the $\delta^2\text{H}$ values are higher – for both before and after extraction – than for the $\delta^{18}\text{O}$ values before and after extraction.

All in all, the measures of dispersion are similar for the $\delta^2\text{H}$ values before and after extraction and for the $\delta^{18}\text{O}$ values before and after extraction, which underlines the statistical equality. This leads to the conclusion that the constructed vacuum extraction device did not affect the water isotopic signature of the extracted water and, thus, no isotope fractionation occurred during the extraction.

However, measures of dispersion of the $\delta^2\text{H}$ values tend to be slight different from the $\delta^{18}\text{O}$ values. This fact could be due to an inaccurate measuring of the LGR DLT-100, since all samples were treated equally before, during, and after the extraction procedure. In order to check for severe analytical errors of the LGR DLT-100, always two sub-samples of the same extracted water, from the same collection tube, were analysed and averaged. In addition, measurements were repeated when the results of the samples differed widely. However, the LGR DLT-100 is very sensitive in regard to surrounding temperature conditions and temperature has not been constant over the whole measuring period. In addition, working with extremely low concentrations of the reference standard can also result in measuring inaccuracies of the LGR DLT-100.

Overall, the slight differences in the isotopic signatures, which should be detected in all validation experiments, may not be measured whether with the LGR DLT-100, nor with another similar Water Isotope Analyser – for instance the PICARRO L1102-*i* (PICARRO Inc., 480 Oakmead Parkway, Sunnvale, CA, 94085, US), which is indeed more stable in regard to the surrounding temperature, but which also has similar detection limits (about 0.1 [‰] for $^{18}\text{O}/^{16}\text{O}$ and 0.5 [‰] for $^2\text{H}/^1\text{H}$) (L1102-*i* datasheet, 2009). Therefore, it is assumed that the observed deviance of the $\delta^{18}\text{O}$ values is caused by measuring inaccuracy of the LGR DLT-100, even the deviance within the groups of “before extraction”, since always the same water sample was used.

3.2 Effect of the high-purity nitrogen aeration

In validation experiment 2.1, the water isotope signatures of Gießen's tap water after extraction, with and without high-purity nitrogen aeration were compared to test if the nitrogen aeration affects the isotopic composition of the extracted water. Therefore, the data from the extracted water of experiment 1 without high-purity nitrogen aeration were tested against new data from an extraction with high-purity nitrogen aeration with the same type of water. As before, both the $\delta^2\text{H}$ and $\delta^{18}\text{O}$ values of the stable water isotope analysis were separately positively tested for normal distribution (Kolmogorov-Smirnov-test, $p = 0.05$). Hence, t-tests could be performed for the $\delta^2\text{H}$ and $\delta^{18}\text{O}$ values with significance levels α of 5%. The t-tests showed no statistically significant differences in the $\delta^2\text{H}$ and $\delta^{18}\text{O}$ values with and without high-purity nitrogen aeration. This is additionally underlined by the means and medians, which are nearly the same for the $\delta^2\text{H}$ and $\delta^{18}\text{O}$ values of the groups with and without high-purity nitrogen aeration (Table 5).

Table 5: Descriptive statistics of the $\delta^2\text{H}$ and $\delta^{18}\text{O}$ values [‰] with/without high-purity nitrogen aeration for validation experiment 2.1.

Measures of dispersion	$\delta^2\text{H}$		$\delta^{18}\text{O}$	
	without high-purity nitrogen aeration	with high-purity nitrogen aeration	without high-purity nitrogen aeration	with high-purity nitrogen aeration
Mean	-57.66 [‰]	-58.51 [‰]	-9.38 [‰]	-9.33 [‰]
Median	-57.61 [‰]	-58.51 [‰]	-9.33 [‰]	-9.34 [‰]
Variance	2.13	0.24	0.09	0.01
Standard deviation	1.46	0.41	0.30	0.08
Minimum	-59.41 [‰]	-59.14 [‰]	-9.84 [‰]	-9.45 [‰]
Maximum	-55.70 [‰]	-57.88 [‰]	-9.05 [‰]	-9.20 [‰]

When comparing the box plots of the $\delta^2\text{H}$ and $\delta^{18}\text{O}$ values (Figure 29 and 30) with and without high-purity nitrogen aeration, it is apparent that the ranges of variation are smaller for the groups “with high-purity nitrogen aeration”.

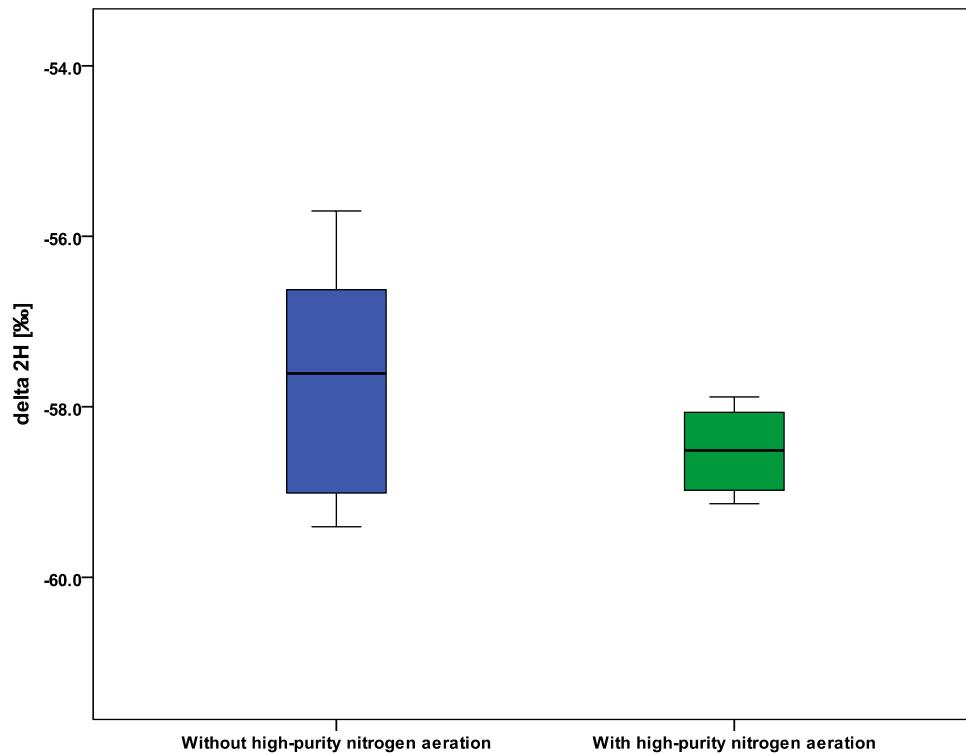


Figure 29: Comparison of the $\delta^2\text{H}$ values of Gießen's tap water after water extraction with and without high-purity nitrogen aeration.

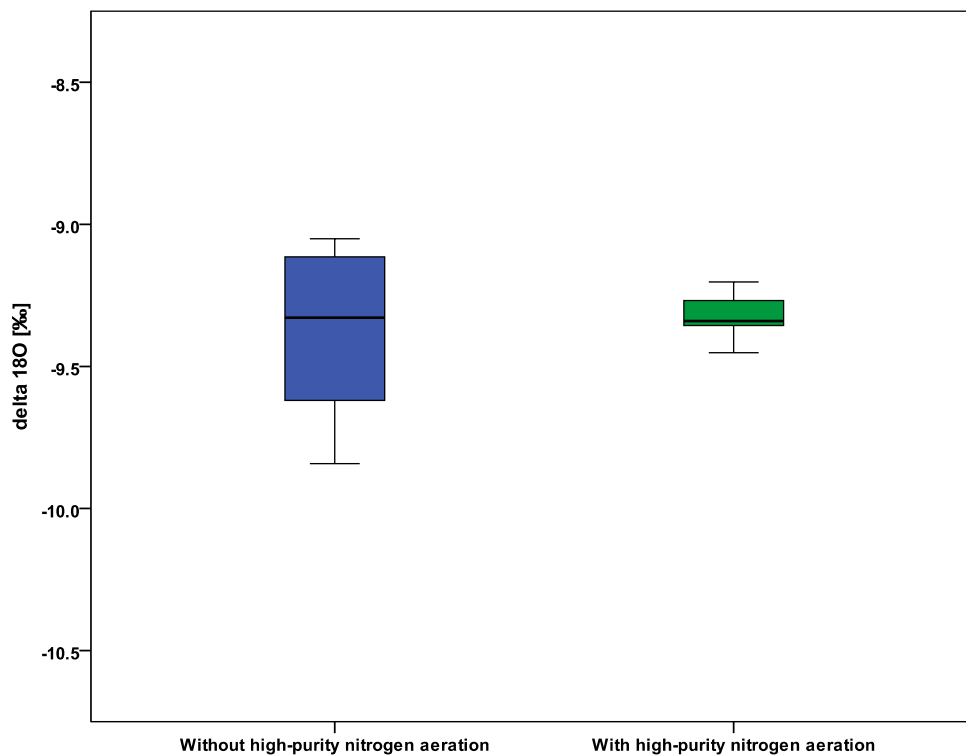


Figure 30: Comparison of the $\delta^{18}\text{O}$ values of Gießen's tap water after water extraction with and without high-purity nitrogen aeration.

The greatest and the smallest values of these groups ($\delta^{2}\text{H}$ and $\delta^{18}\text{O}$) are not far off the 50% of the values inside the box plots. It can be inferred that high-purity nitrogen aeration did not affect the isotopic signatures of the extracted waters, but decreased the variance of the values. For the group “without high-purity nitrogen aeration” the $\delta^{2}\text{H}$ values showed a variance of 2.13 and the $\delta^{18}\text{O}$ values of 0.09. In comparison, the variances of the group “with high-purity nitrogen aeration” for $\delta^{2}\text{H}$ values are: 0.24 and for $\delta^{18}\text{O}$ values: 0.01. This concludes that high-purity nitrogen aeration can contribute to a better distribution of the values and, therefore, to a higher accuracy and reliability of the values. As expected, the aeration with nitrogen gas, which is an inert gas, did not affect the isotopic composition of the extracted water. Therefore, it is used in the following validation experiments as a protective layer above the extracted water to minimise the risk of evaporation during defrosting and to reduce the risk of a mixture of the extracted sample water with atmospheric water vapour.

To verify the results of experiment 2.1, a second experiment with the same procedure but different test water (Schwingbach water) was conducted (test 2.2). Therefore, the five original samples of Schwingbach water, which did not undergo water extraction process before, and the twelve extracted water samples with high-purity nitrogen aeration after the extraction – averaged over the two sub-samples collected from the same U-tube – were compared. Likewise, the $\delta^{2}\text{H}$ and $\delta^{18}\text{O}$ values of the stable water isotope analysis were separately positively tested for normal distribution (Kolmogorov-Smirnov-test, $p = 0.05$). Again t-tests could be performed with significance levels α of 5%. The statistics showed no significant differences in the $\delta^{2}\text{H}$ of Schwingbach water before and after water extraction with high-purity nitrogen aeration. For the $\delta^{18}\text{O}$ values of Schwingbach water, slight statistically differences ($p = 0.04$) were observed comparing the values before and after extraction with high-purity nitrogen aeration.

Table 6 shows the descriptive statistics for the comparison of the $\delta^{2}\text{H}$ and $\delta^{18}\text{O}$ values of Schwingbach water, before and after water extraction, with high-purity nitrogen aeration. Again, the means of the samples before and after extraction were similar for both $\delta^{2}\text{H}$ (before extraction: -56.01 [‰], after extraction: -55.52 [‰]) and $\delta^{18}\text{O}$ values (before extraction: -8.46 [‰], after extraction: -8.76 [‰]), even if minor statistically differences were observed for the $\delta^{18}\text{O}$ values.

When comparing the box plots of the $\delta^{2}\text{H}$ and $\delta^{18}\text{O}$ values (Figure 31 and 32) before and after extraction with high-purity nitrogen aeration, it is apparent that the ranges of variation are smaller for the groups after extraction with high-purity nitrogen aeration.

Table 6: Descriptive statistics of the $\delta^2\text{H}$ and $\delta^{18}\text{O}$ values of Schwingbach water before and after water extraction with high-purity nitrogen aeration for validation experiment 2.2.

Measures of dispersion	$\delta^2\text{H}$		$\delta^{18}\text{O}$	
	Before extraction	After extraction	Before extraction	After extraction
Mean	-56.01 [‰]	-55.52 [‰]	-8.46 [‰]	-8.76 [‰]
Median	-56.50 [‰]	-55.56 [‰]	-8.42 [‰]	-8.79 [‰]
Variance	2.58	0.49	0.10	0.07
Standard deviation	1.61	0.61	0.32	0.27
Minimum	-57.97 [‰]	-56.57 [‰]	-8.78 [‰]	-9.03 [‰]
Maximum	-54.23 [‰]	-54.55 [‰]	-8.02 [‰]	-8.36 [‰]

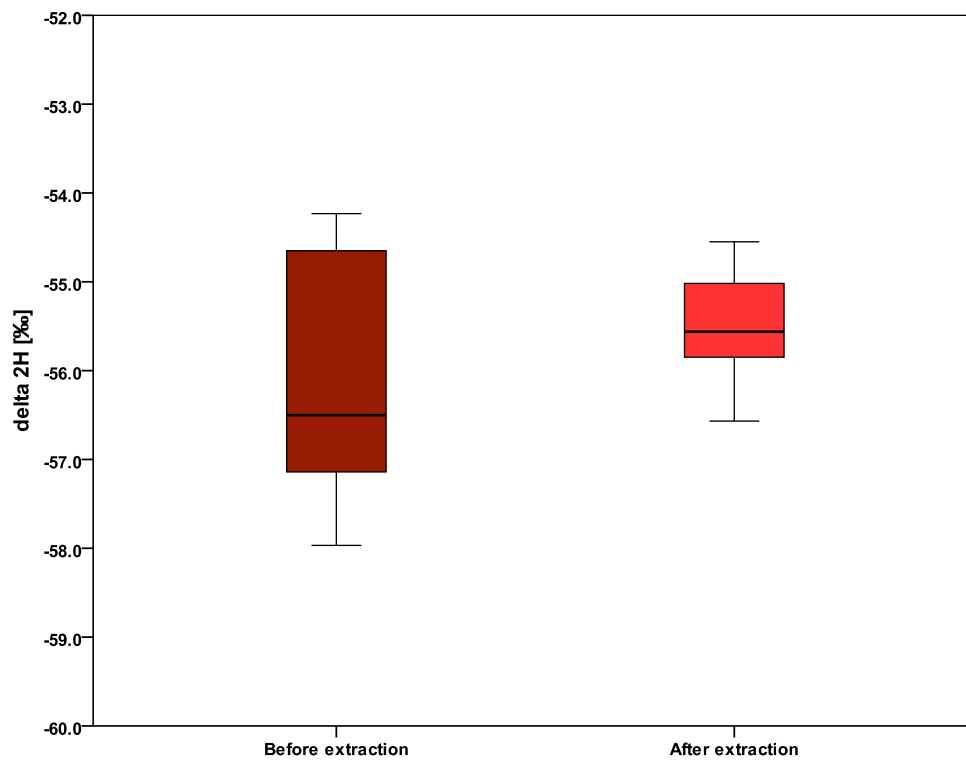


Figure 31: Comparison of the $\delta^2\text{H}$ values of Schwingbach water before and after water extraction with high-purity nitrogen aeration.

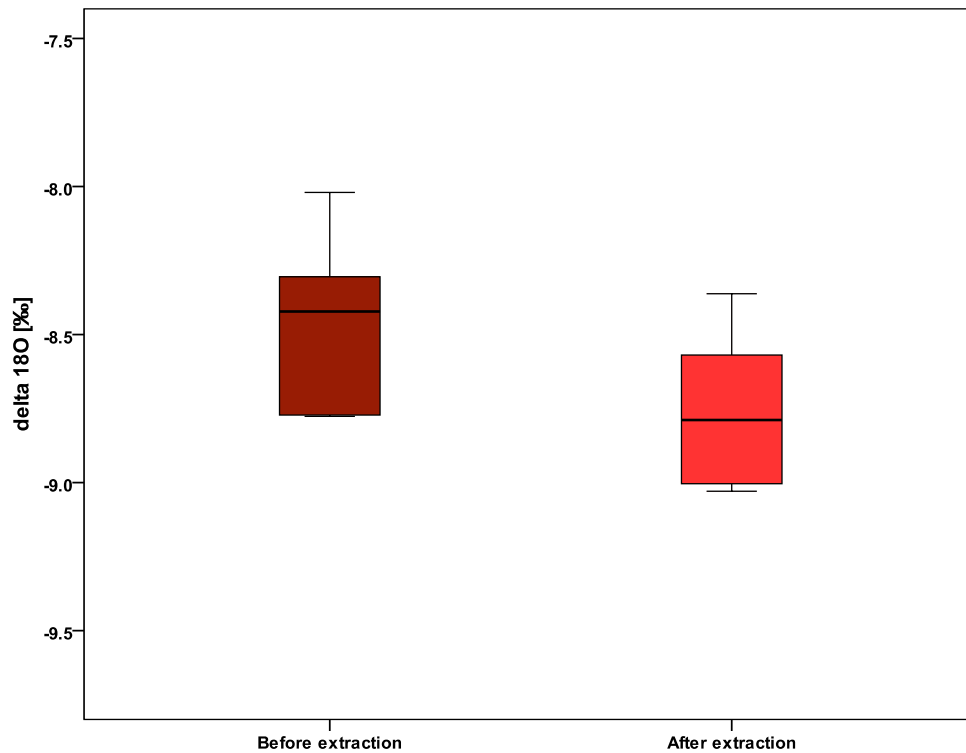


Figure 32: Comparison of the $\delta^{18}\text{O}$ values of Schwingbach water before and after water extraction with high-purity nitrogen aeration.

Likewise, the slight statistically significant differences in the $\delta^{18}\text{O}$ values can be ascribed to the measuring inaccuracy, respectively to the detection limit of the LGR DLT-100, which is not optimal for the aims of the validation experiments. Underlining this fact, the $\delta^2\text{H}$ and $\delta^{18}\text{O}$ values for the groups “before extraction” should not differ much within their group because they are taken from the same water sample.

3.3 Cross-contamination test among the extraction units

The aim of validation experiment 3 was to test, if cross-contamination among the six extraction units occurs. Therefore, three extraction tubes were filled with Schwingbach water and the other three with precipitation from Gießen during the same extraction process. Schwingbach water and precipitation from Gießen were chosen to be compared during the same extraction process because their water isotopic signatures already differ strongly a priori.

After water extraction two water samples were collected from every U-tube (six from precipitation from Gießen collected from the first three U-tubes and six samples of Schwingbach water collected from the other three U-tubes) and analysed via the LGR DLT-100. A higher sample size could not be achieved due to the limited number of six extractions- (U-tubes).

The data of the two sub-samples from each U-tube was averaged, so that the three means of the extracted precipitation from Gießen could be compared to the three means of the extracted Schwingbach water.

These data were separately tested for normal distribution (Shapiro-Wilk-test, $p = 0.05$), which was given for the $\delta^2\text{H}$ and $\delta^{18}\text{O}$ values of Schwingbach water and precipitation from Gießen. Hence, t-tests could be performed to test the $\delta^{18}\text{O}$ values of Schwingbach water against the precipitation from Gießen and to test the $\delta^2\text{H}$ values of Schwingbach against the precipitation from Gießen. Both tests revealed highly statistically significant differences between Schwingbach water and precipitation from Gießen in terms of their water isotopic signatures after extraction. The statistically significant differences at the $p < 0.01$ level (***) between these two types of water after extraction are visualised by the box plots of the isotopic signatures of Schwingbachs water and the precipitations from Gießen (Figure 33 and 34). As shown in Table 7, the medians of $\delta^2\text{H}$ and $\delta^{18}\text{O}$ values of Schwingbach water strongly differ with the medians of precipitation from Gießen, which underlines the statistical difference between these two types of water after extraction.

Table 7: Descriptive statistics of the $\delta^2\text{H}$ and $\delta^{18}\text{O}$ values of precipitation from Gießen and Schwingbach water after water extraction for validation experiment 3.

Measures of dispersion	$\delta^2\text{H}$		$\delta^{18}\text{O}$	
	Precipitation from Gießen	Schwingbach water	Precipitation from Gießen	Schwingbach water
Mean	-1.47 [‰]	-56.69 [‰]	-1.32 [‰]	-8.81 [‰]
Median	-1.46 [‰]	-56.99 [‰]	-1.32 [‰]	-8.81 [‰]
Variance	0.03	0.21	0.00	0.03
Standard deviation	0.17	0.54	0.04	0.19
Minimum	-1.65 [‰]	-57.02 [‰]	-1.36 [‰]	-9.11 [‰]
Maximum	-1.31 [‰]	-56.06 [‰]	-1.28 [‰]	-8.77 [‰]

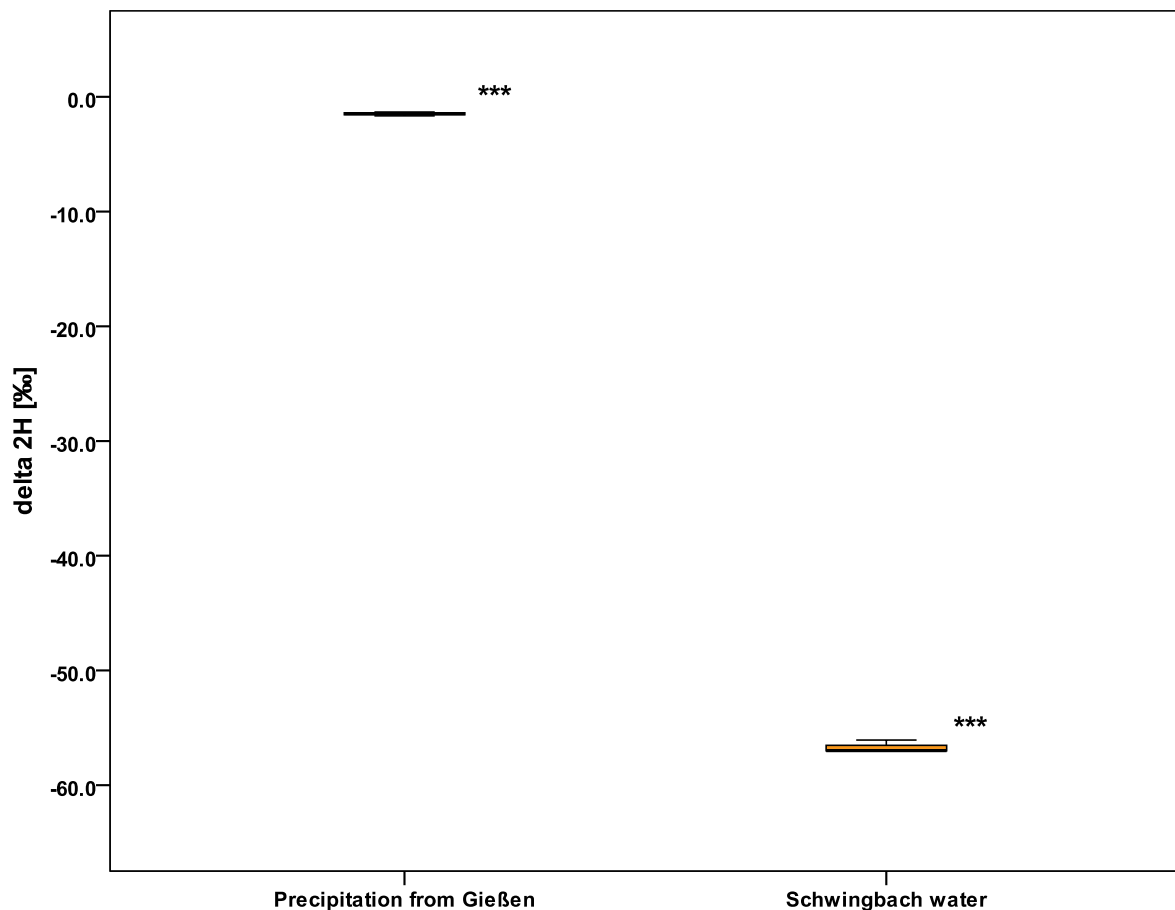


Figure 33: Comparison of the $\delta^2\text{H}$ values of precipitation from Gießen and Schwingbach water after the same water extraction procedure with high-purity nitrogen aeration.

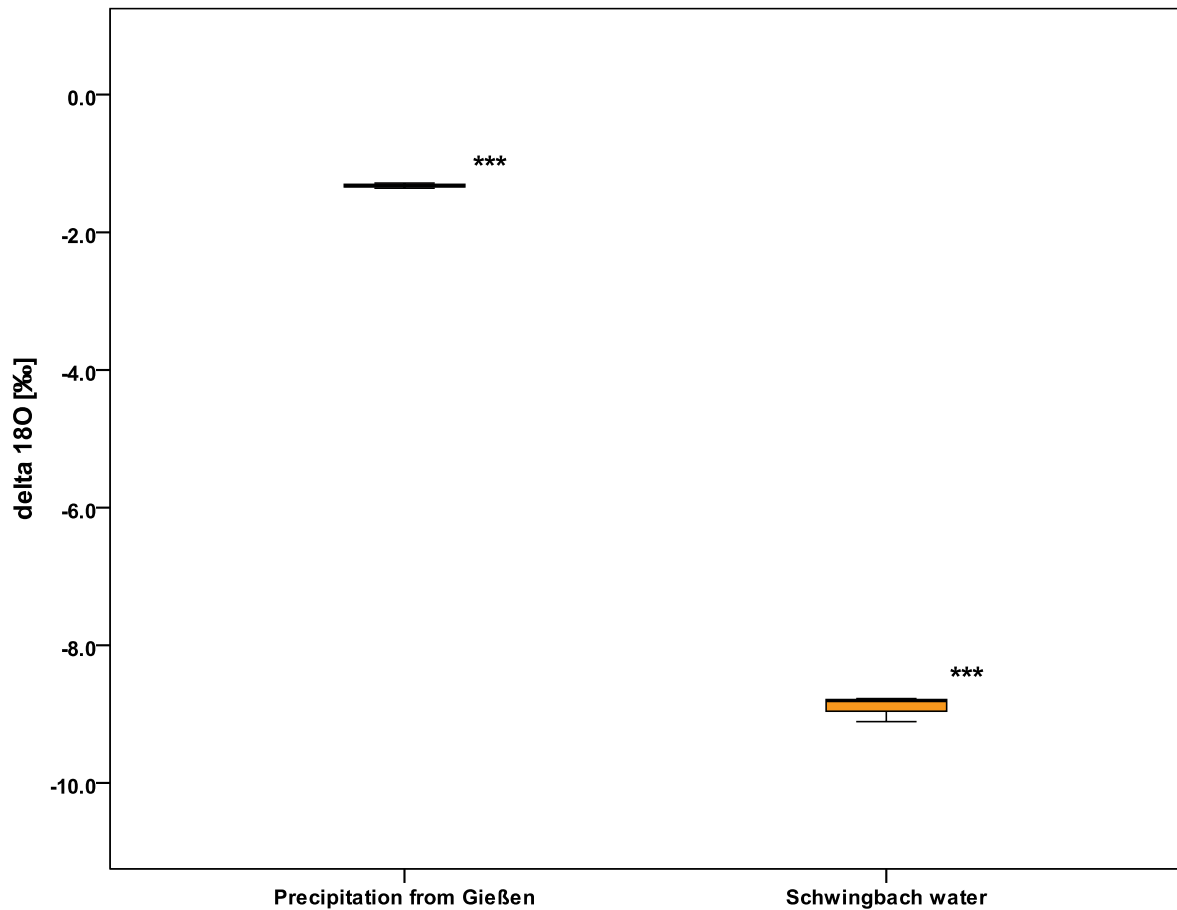


Figure 34: Comparison of the $\delta^{18}\text{O}$ values of precipitation from Gießen and Schwingbach water after the same water extraction procedure with high-purity nitrogen aeration.

The standard deviations and variances of the $\delta^2\text{H}$ and the $\delta^{18}\text{O}$ values of both water types are very small, meaning that the minimum and maximum are not far apart. Additionally, no outliers in the distributions of Schwingbach water and precipitation from Gießen occurred, which would have been arisen when cross-contamination among the extraction units took place. For this reason, validation experiment 3 demonstrated that there is no cross-contamination among the extraction units during water extraction process and, therefore, the six extraction units are working independently.

4. Concluding remarks and outlook

The validation experiments conclude that neither the vacuum extraction procedure itself nor the high-purity nitrogen aeration leads to a modified isotopic composition of the extracted test waters (validation experiments 1 to 2) in the new cryogenic vacuum extraction device at the ILR.

Withdrawing the atmosphere before starting the water extraction process eliminates the error caused by a potential mixing of the atmospheric water vapour with the extracted water during the extraction procedure.

In addition, validation experiment 1 shows that the extraction units are vacuum-tight. If the extraction device was not vacuum-tight, it would lead to a loss of pressure and an incomplete water extraction resulting in modified water isotopic signatures after the extraction process. Furthermore, validation experiment 3 concludes that the extraction units are working independently without cross-contamination. The constructed aeration with high-purity nitrogen gas is a feasible option to minimise the risk of evaporative water loss by situating a protective layer of gas on the extracted defrosting water. Instead of an aeration of the vacuum system with atmospheric air, it does not mix up with the extracted water, and, consequently, does not modify the isotopic composition of the extracted sample water.

The spread of the $\delta^{2}\text{H}$ and $\delta^{18}\text{O}$ values is probably due to measuring inaccuracy of the LGR DLT-100, which can, for instance, be minimised by an improved temperature control during the isotope analysis process. The water isotopic analysis could have also been performed using a similar Water Isotope Analyser, for instance the PICARRO L1102-*i*, which is indeed more stable in regard to the surrounding temperature, but which also has similar detection limits (about 0.1 [‰] for $^{18}\text{O}/^{16}\text{O}$ and 0.5 [‰] for $^{2}\text{H}/^{1}\text{H}$) (L1102-*i* datasheet, 2009). Consequently, the spread of the $\delta^{2}\text{H}$ and $\delta^{18}\text{O}$ values, which occurred using the LGR DLT-100, would probably also occur with another analyser.

Summarising, the constructed cryogenic vacuum water extraction device guarantees stable extraction conditions and can be applied in stable isotope research science.

For extracting more than six samples simultaneously, a stainless steel fork as it is already used at the PSI (Figure 35) could be constructed and adapted for the ILR's extraction device.

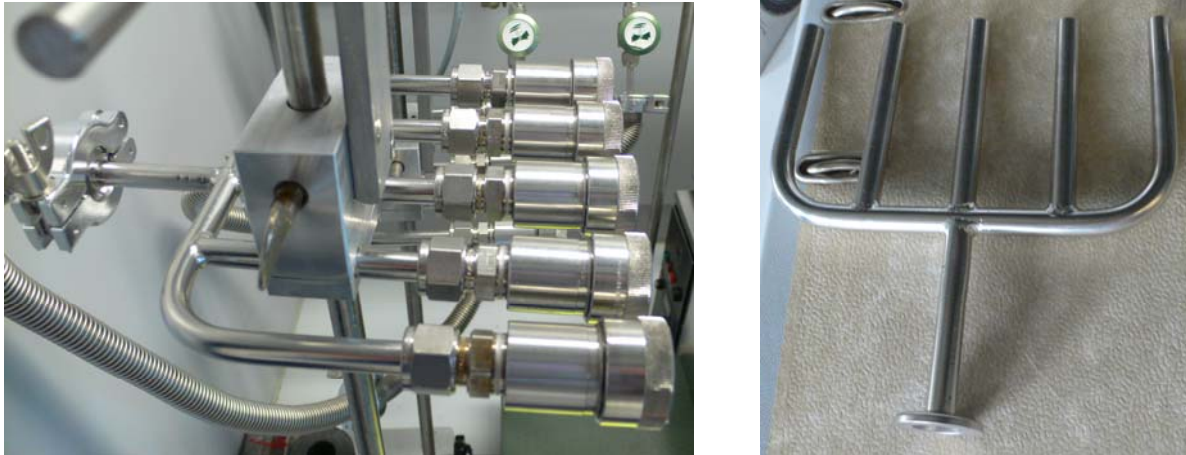


Figure 35: Photography of fiver extraction unit used at the PSI (Own source).

This fork consists of five short tubular extraction arms and has a stainless steel flange at its end, which can easily be connected to a flexible hose. For instance, it can be connected to the KF Swagelok-adapters, which are attached on the one side to the union tee fittings via short connection tubes. The flange-flange connection to the fiver extraction unit can be generated via centering- and clamp rings. The five short tubular arms of the fork can then be equipped with KF Swagelok-adapters and be attached to the flexible hoses with the extraction-collection unit at the other end.

However, a disadvantage of such a construction is that one diaphragm valve would be used to apply, i. e. shut down the vacuum for five extraction tubes at one go. In addition, one sample can never more be extracted alone. Probably, a higher vacuum has to be applied, if the fiver unit is attached to all of the six outgoing and, if thirty samples are extracted simultaneously. Additionally, the attached fiver units have to be tested for a potential cross-contamination as it was performed for the six independent extraction units in this thesis. However, extracting thirty samples during one extraction procedure offers a great time saving.

5. Abstract

Against the background of increasing use of stable water isotopes in hydrogeochemical research sciences, the Institute of Landscape Ecology and Resources Management (ILR) constructed a cryogenic vacuum extraction device. With the principle of cryogenic vacuum extraction, it is possible to determine the isotopic signature of environmental water, more precisely, of soil and plant water serving as pools of local water cycles by extracting their water under vacuum. In the extraction process, the sample is heated under a defined vacuum, which leads to a water evaporation from the soil, i. e. plant sample. Afterwards, the evolved vapour is frozen in a liquid nitrogen (cryogenic) cold trap (Ingraham and Shadel, 1992). After defrosting the obtained sample water, its isotopic signature is analysed via diode laser absorption spectroscopy (Los Gatos Research DLT-100- Liquid Water Isotope Analyser, Los Gatos Research Inc., 67 East Evelyn Avenue, Suite 3, Mountain View, CA, 94041-1529, US).

Among the existing water extraction methods for soil and plant samples, cryogenic vacuum extraction is one of the most widely used methods (Peters and Yakir, 2008).

Hence, the aim of this thesis was to create a vacuum-tight, reliable, and user-friendly cryogenic vacuum extraction device with an extendable modularity and several independently working extraction units for application in stable water isotope research science and, furthermore, to specify this apparatus through validation experiments.

The constructed vacuum extraction device of the ILR is mainly based on the principle used by West et al. (2006) and by the Paul Scherrer Institute (PSI, Villigen, CH). Implying that an apparatus with independently working extraction units - basically consisting of stainless steel Swagelok® fittings for realising the vacuum-tightness and glassware for a visual observation of the extraction process - was build.

Beyond the execution of the existing devices, the extraction apparatus is additionally equipped with a mechanism for high-purity nitrogen aeration. This execution prevents the loss of water vapour during defrosting after extraction by purging every sample with high-purity nitrogen gas after the water extraction procedure. Moreover, the aeration of the vacuum system with high-purity nitrogen gas instead of aeration with atmospheric air, overcomes the risk of a mixture of atmospheric water vapour with the extracted sample water. Nitrogen gas, as an inert gas, does not react with the extracted water, but serves as a protective layer over the extracted defrosting sample water, minimising the error of isotope fractionation.

The new vacuum extraction device was tested in order to specify it. The concern of the validation experiments was to examine whether the water isotopic signature is changed through the extraction process, whether the high-purity nitrogen aeration affects the water isotopic composition, and whether cross-contamination among the six extraction units occurs.

All validation tests were conducted with water – three different types of water with known isotopic composition - instead of soil or plant material for an easier implementation of the experiments and better comparability of the results.

The validation experiments revealed that the constructed cryogenic vacuum extraction device is vacuum-tight and, consequently, there was no change in the isotopic signature of the extracted water due to a complete water extraction process. As expected, the high-purity nitrogen aeration after the water extraction did not change the isotopic signature of the extracted sample water, but could contribute to a better distribution of the values for the water isotopic signatures and, therefore, to a higher accuracy. Finally, while extracting two different types of water during one extraction process, no exchange among these waters could be observed, concluding that no cross-contamination among the six independent extraction units occurred. Summarising, the constructed cryogenic vacuum water extraction device guarantees stable extraction conditions. Thus, this apparatus is a proper tool to be applied in water isotope research sciences.

6. Zusammenfassung

Vor dem Hintergrund der zunehmenden Anwendung stabiler Wasserisotope in hydrogeochemischen Untersuchungen wurde eine kryogene Vakuumextraktionsanlage am Institut für Landschaftsökologie und Ressourcenmanagement (ILR) errichtet. Mit der kryogenen Vakuumextraktion ist es möglich, die Isotopensignatur von Umweltwasser bestimmen zu können, genauer von Boden- und Pflanzenwasser als Pools lokaler Wasserkreisläufe, durch die Extraktion ihres Wassers unter Vakuum. Dabei wird die zu extrahierende Probe unter einem angelegten Druck erhitzt, wodurch das Wasser aus der Boden- bzw. Pflanzenprobe evaporiert. Anschließend wird es in einer Flüssigstickstoff-Kühlfalle (kryogen) ausgefroren (Ingraham and Shadel, 1992). Nach dem Auftauen des erhaltenen Probenwassers, kann seine Isotopensignatur mittels Diodenlaser Absorptionsspektroskopie (Los Gatos Research DLT-100- Liquid Water Isotope Analyser, Los Gatos Research Inc., 67 East Evelyn Avenue, Suite 3, Mountain View, CA, 94041-1529, US) bestimmt werden.

Unter den existierenden Wasserextraktionsverfahren für Boden- und Pflanzenproben ist die kryogene Vakuumextraktion eine der meist verwendeten Methoden (Peters and Yakir, 2008). Demzufolge war das Ziel dieser Arbeit, eine vakuumdichte, verlässliche und benutzerfreundliche kryogene Vakuumextraktionsanlage mit einer erweiterbaren Modularität und unabhängig voneinander arbeitenden Extraktionseinheiten für den Einsatz in der stabilen Wasserisotopenforschung zu errichten und darüber hinaus diese Anlage durch Validierungsversuche zu spezifizieren.

Die konstruierte Wasserextraktionsanlage des ILR basiert hauptsächlich auf dem Prinzip, welches von West et al. (2006) und am Paul Scherrer Institut (PSI, Villigen, CH) praktiziert wird. Dieses Prinzip impliziert, dass die Vakuumextraktionsanlage mit sechs unabhängig voneinander arbeitenden Extraktionseinheiten ausgestattet ist, die hauptsächlich aus Swagelok®-Stahlverschraubungen für die Vakuumdichtigkeit besteht sowie aus Glas für eine einfachere visuelle Überwachung des Extraktionsprozesses.

Über die bereits bestehenden Anlagenbauten hinaus, verfügt die Wasserextraktionsanlage des ILR über eine Einrichtung zur Belüftung des Vakuumsystems mit hochreinem Stickstoffgas. Diese Ausstattung verhindert den evaporativen Wasserverlust während des Auftauens des extrahierten Wassers durch die Begasung jeder gewonnenen Wasserprobe mit hochreinem Stickstoffgas nach der Wasserextraktion. Darüber hinaus überwindet eine Belüftung mit hochreinem Stickstoffgas, anstelle einer Belüftung des Vakuumsystems mit Atmosphärenluft, das

Risiko der Vermischung von atmosphärischem Wasserdampf mit dem extrahierten Probenwasser. Stickstoff ist ein inertes Gas, welches nicht mit dem extrahierten Wasser reagiert, aber als schützende Schicht über dem auftauenden Extraktionswasser dienen kann und damit den Fehler der Isotopenfraktionierung minimieren kann.

Nach dem eigentlichen Aufbau der Vakuumextraktionsanlage wurde diese anhand von Validierungstest spezifiziert. Dabei sollte herausgefunden werden, ob die Wasserisotopensignatur durch den Extraktionsprozess verändert wird, ob die Belüftung mit Stickstoffgas die Wasserisotopenzusammensetzung beeinflusst und ob Querkontaminationen zwischen den sechs Extraktionseinheiten auftreten. Für eine einfachere Realisierung und eine bessere Vergleichbarkeit der Ergebnisse wurden alle Testversuche mit drei verschiedenen Wasserarten bekannter Isotopensignatur anstelle von Boden- oder Pflanzenproben durchgeführt.

Die Validierungsversuche ergaben, dass die errichtete kryogene Extraktionsanlage vakuumdicht ist und daher aufgrund eines vollständigen Extraktionsprozesses keine Veränderungen der Isotopensignaturen des extrahierten Wassers auftraten. Wie erwartet, fand auch durch die Belüftung mit Stickstoffgas, keine Beeinflussung der Wasserisotopensignaturen des gewonnenen Probenwassers statt. Sie kann jedoch zu einer besseren Verteilung der Wasserisotopenwerte beitragen und damit zu einer höheren Genauigkeit der Ergebnisse. Schließlich konnte durch die parallele Extraktion zweier Wasserarten während eines Extraktionsprozesses herausgefunden werden, dass es zu keiner Vermischung des Probenwassers und damit keinen Querkontaminationen zwischen den einzelnen Extraktionseinheiten kommt.

Zusammenfassend garantiert die kryogene Vakuumextraktionsanlage des ILR stabile Extraktionsbedingungen. Durch die Validierungsversuche konnte die einwandfreie Funktionalität bestätigt werden. Damit ist die kryogene Vakuumextraktionsanlage ein geeignetes Wasserextraktionsgerät für den Einsatz in der stabilen Wasserisotopenforschung.

7. References

- Aggarwal, P. K., Gat, J. R., Fröhlich, K. F. O. (2007): *Isotopes in the water cycle: past present and future of a developing science*, International Atomic Energy Agency (IAEA), Springer Verlag, New York
- Araguas-Araguas, L., Froehlich, K., Rozanski, K. (2000): Deuterium and oxygen-18 isotope composition of precipitation and atmospheric moisture, *Hydrological Processes* 14, 1341 – 1355
- Baertschi, P. (1976): Absolute ^{18}O content of standard mean ocean water, *Earth and Planetary Science Letters* 31, 341 – 344
- Barnes, C. J., Allison, G. B. (1988): Tracing of water movement in the unsaturated zone using stable isotopes of hydrogen and oxygen, *Journal of Hydrology* 100, 143 – 176
- Berman, E. S. F., Gupta, M., Gabrielli, C., Garland, T., McDonnell, J. J. (2009): High-frequency field-deployable isotope analyzer for hydrological applications, *Water Resources Research* 45, doi: 10.1029/2009WR008265
- Boutton, T. W., Yamasaki, S. (1996): *Mass spectrometry of soils*, Marcel Dekker, New York
- Clark, I., Fritz, P. (1997): *Environmental isotopes in hydrogeology*, CRC Press LLC, Florida
- Cook, P., Herczeg, A. L. (2000): *Environmental Tracers in Subsurface Hydrology*, therein: Coplen, T. B., Herczeg, A. L., Barnes, C.: *Isotope engineering: Using stable isotopes of the water molecule to solve practical problems*, Kluwer Academic Publishers, Boston
- Craig, H. (1961a): Isotopic variations in meteoric waters, *Science* 133, 3465, 1702 – 1703
- Craig, H. (1961b): Standard for reporting concentrations of deuterium and oxygen-18 in natural waters, *Science* 133, 3467, 1833 – 1834

- Dalton, F. N. (1988): Plant root water extraction studies using stable isotopes, *Plant and Soil* 111, 217 – 221
- Dawson, T. E., Ehleringer, J. R. (1993): Isotopic enrichment of water in „woody“ tissues of plants: Implications for plant water source, water uptake, and other studies which use the stable isotopic composition of cellulose, *Geochimica et Cosmochimica Acta* 57, 3487 – 3492
- Dawson, T. E., Mambelli, St., Plamboeck, A. H., Templer, P. H., Tu, K. P. (2002): Stable isotopes in plant ecology, *Annual Revue of Ecological Systems* 33, 507 – 559
- Delta F Corporation, Moisture Analyser (2010): <http://www.delta-f.com/moisture.html>, last page view: 04/01/2010
- Ehleringer, J. R., Dawson, T. E. (1992): Water uptake by plants: perspectives from stable isotope composition, *Plant, Cell and Environment* 15, 1073 – 1082
- EPA: United States Environmental Protection Agency (2009): <http://www.epa.gov/wed/pages/isirf/AP02Final.pdf>, last page view: 19/12/09
- Gat, J. R. (1996): Oxygen and hydrogen isotopes in the hydrologic cycle, *Annual Review Earth Planet Science* 24, 225 – 62
- Ghosh, P., Brand, W. A. (2003): Stable isotope ratio mass spectrometry in global climate change, *International Journal of Mass Spectrometry* 228, 1 – 33
- Hagemann, R., Nief, G., Roth, E. (1970): Absolute isotopic scale for deuterium, analysis of natural water: Absolute D/H ratio for SMOW, *Tellus* 22, 712 – 715
- Hoefs, J. (2009): *Stable isotope geochemistry*, 6th Edition, Springer Verlag, Berlin
- Ingraham, N. L., Shadel, C. (1992): A comparison of the toluene distillation and vacuum/heat methods for extracting soil water for stable isotopic analysis, *Journal of Hydrology* 140, 371 – 387

Kendall, C., McDonnell, J. J. (1998): Isotope Tracers in Catchment Hydrology, Elsevier Science B.V., Amsterdam

Kerstel, E. R. Th., Gagliardi, G., Gianfrani, L., Meijer, H. A. J., Trigt, van, R., Ramaker, R. (2002): Determination of the $^2\text{H}/^1\text{H}$, $^{17}\text{O}/^{16}\text{O}$, and $^{18}\text{O}/^{16}\text{O}$ isotope ratios in water by means of tunable diode laser spectroscopy at 1.39 μm , Spectrochimica Acta Part A 58, 2389 – 2396

LGR: Los Gatos Research, Liquid Water Isotope Analyser Manual (2010): https://snri.ucmerced.edu/snri/eal/Liquid%20Water%20Manual_091908.pdf, last page view: 21/02/2010

L1102-*i* datasheet: PICARRO, Water Isotope Analyser (2009): http://www.picarro.com/assets/docs/water_isotopes_liquid_datasheet.pdf, last page view: 04/05/2010

Lis, G., Wassenaar, L. I., Hendry, M. J. (2008): High-precision laser spectroscopy D/H and $^{18}\text{O}/^{16}\text{O}$ measurements of microliter natural water samples, Analytical Chemistry 80, 287 – 293

McMaster, M. C. (2008): GC/MS: A practical user's guide, 2nd. Edition, John Wiley & Sons, Hoboken, New Jersey

IAEA: International Atomic Energy Agency (2010a): http://www-naweb.iaea.org/naweb/ih/document/global_cycle/vol%20I/cht_i_03.pdf, last page view: 18/12/2009

IAEA: International Atomic Energy Agency (2010b): http://www-naweb.iaea.org/naweb/ih/document/global_cycle/vol%20II/cht_ii_02.pdf, last page view: 18/12/2009

Otieno, D. O., Kurz-Besson, C., Liu, J., Schmidt, M. W. T., Vale-Lobo do, R., David, T. S., Siegwolf, R., Pereira, J. S., Tenhunen, J. D. (2006): Seasonal variations in soil and plant water status in a *Quercus suber* L. stand: roots as determinants of tree productivity and survival in the Mediterranean-type ecosystem, Plant and Soil 283, 119 – 135

Peters, L. I., Yakir, D. (2008): A direct and rapid leaf water extraction method for isotopic analysis, *Rapid Communications in Mass Spectrometry* 22, 2929 – 2936

Poage, M. A., Chamberlain, C. P. (2001): Empirical relationships between elevation and the stable isotope composition of precipitation and surface waters: Considerations for studies of paleoelevation change, *American Journal of Science* 301, 1 – 15

Revesz, K., Woods, P. H. (1990): A method to extract soil water for stable isotope analysis, *Journal of Hydrology* 115, 397 – 406

Rundel, P. W., Ehleringer, J. R., Nagy, K. A. (1989): *Stable Isotopes in Ecological Research*, Ecological Studies 68, Springer Verlag, New York

Sacchi, E., Michelot, J.-L., Pitsch, H., Lalieux, P., Aranyossy, J.-F. (2001); Extraction of water and solutes from argillaceous rocks for geochemical characterisation: Methods, processes, and current understanding, *Hydrogeology Journal* 9, 17 – 33

SAHRA: Sustainability of semi-Arid Hydrology and Riparian Areas (2010):

<http://www.sahra.arizona.edu/programs/isotopes/oxygen.html#9>, last page view: 21/02/2010

Sala, O. E., Jackson, R. B., Mooney, H. A., Howarth, R. W. (2000): *Methods in Ecosystem Science*, therein: Ehleringer, J. R., Roden, J., Dawson, T. E.: Assessing ecosystem-level water relations through stable isotope ratio analyses, Springer Verlag, New York

Seiler, K.-P., Gat, J. R. (2007): *Groundwater recharge from run-off, infiltration and percolation*, water science and technology library, Springer Verlag, New York

University of Kwazulu-Natal, Geography seminar, (2003):

http://www.geography.ukzn.ac.za/seminars/oxygen_isotopes.pdf, last page view: 21/02/2010

University of Utah, Isotope course (2009):

http://ecophys.biology.utah.edu/public/Isotope_course_readings/Dawson.SIE-2009.pdf, last page view: 29/11/2009

Unkovich, M., Pate, J., McNeill, A., Gibbs, D.J. (2001): Stable isotope techniques in the study of biological processes and functioning of ecosystems, Fundamentals of stable isotope chemistry and measurement, Kluwer Academic Publishers, Netherlands

Vendramini, P. F., Sternberg, L. da, S. L. (2007): A faster plant stem-water extraction method, Rapid Communications in Mass Spectrometry 21, 164 – 168

Wang, L., Caylor, K. K., Dragoni, D. (2009): On the calibration of continuous, high-precision $\delta^{18}\text{O}$ and $\delta^2\text{H}$ measurements using an off-axis integrated cavity output spectrometer, Rapid Communications in Mass Spectrometry 23, 530 – 536

Wang, X.-F., Yakir, D. (2000): Using stable isotopes of water in evapotranspiration studies, Hydrological Processes 14, 1407 – 1421

West, A. G., Patrickson, S. J., Ehleringer, J. R. (2006): Water extraction times for plant and soil materials used in stable isotope analysis, Rapid Communications in Mass Spectrometry 20, 1317 – 1321

White, J. W. C., Cook, E. R., Lawrence, J. R., Broecker, W. S. (1985): The D/H ratios of sap in trees; implications for water sources and tree ring D/H ratios, Geochimica et Cosmochimica Acta 49, 237 – 246

Yakir, D. (2000): The use of stable isotopes to study ecosystem gas exchange, Oecologia, 123, 297 – 311

8. Appendix

8.1 Appendix 1

Table 8: Material list.

Article description	Ordering number	Producer	Distributor	Number	Material	Measurements
diaphragm valve	SS-DLS8MM	Swagelok Company, 29500 Solon Road, 44139, Solon, OH, US	B.E.S.T. Fluidsysteme GmbH, Robert-Bosch-Strasse 20, 63477, Maintal, DE	12	316 L stainless steel (body material)	outer diameter 8 mm
tube fitting, reducer	SS-10M0-R-8M	"	"	18	316 L stainless steel (body material)	outer diameter 10 mm x 8 mm
tube fitting, reducer	SS-8M1-PC-6M	"	"	6	316 L stainless steel (body material)	outer diameter 8 mm x 6 mm
tube fitting, reducer	SS-6M0-6-3M	"	"	6	316 L stainless steel (body material)	outer diameter 6 mm x 3 mm

Article description	Ordering number	Producer	Distributor	Number	Material	Measurements
seamless stainless steel tubing (vacuum manifold)	316TI-T10M-S-1.5M-6ME	Swagelok Company, 29500 Solon Road, 44139, Solon, OH, US	B.E.S.T. Fluidsysteme GmbH, Robert-Bosch- Strasse 20, 63477, Maintal, DE	1	316L stainless steel, seamless, titanium alloyed tubing	outer diameter 10 mm, wall 1.5 mm, 1 m length
tube fitting, union tee	SS-10M0-3	"	"	6	316 L stainless steel (body material)	outer diameter 10 mm
RV5 two stage rotary vane pump	A65301903	Edwards GmbH, Ammerthalstrasse 36, 85551, DE	see producer's adress	1		
oil mist filter, model EMF 10	A46226000	Edwards GmbH, Ammerthalstrasse 36, 85551, DE "	see producer's adress	1		
reducing plug connection, QSM-6-4	153327	Festo AG & Co. KG, Ruiter Strasse 82, 73734 Esslingen, DE	see producer's adress	1	polybutylene terephthalate	outer diameter 6 mm x 4 mm
Y-connector, QSMY-3	153370	"	"	5	"	outer diameter 3 mm

Article description	Ordering number	Producer	Distributor	Number	Material	Measurements
portable dewar, type 27, version B	478-4302	KGW Isotherm, Gablonzer Strasse 6, 76185, Karlsruhe, DE	VWR International GmbH, Hilpertstrasse 20a, 64295, Darmstadt, DE	4	borosilicate glass, stainless steel (body material)	cylindric, volume 2 l, inner diameter 138 mm, height 170 mm
water bath, JB aqua 18, standard	462-8136	Grant Instruments, 601 Rte. 206, Suite 26-730, 08844, Hillsborough, NJ, US	"	1		volume 18 l, width 340 mm, depth 570 mm, height 270 mm
PIRANI vacuum gauge, VAP 5-set (sensor, measuring cable)	188-1130	Vacuubrand GmbH & Co. KG, Alfred-Zippe-Strasse 4, 97877, Wertheim, DE	"	1		0.1 [Pa]
laboratory-trolley	139-9940	Hupfer Metallwerke GmbH & Co. KG, Dieselstrasse 20, 48653, Coesfeld, DE	"	1	316 L stainless steel	width 900 mm, depth 600 mm, height 940 mm

Article description	Ordering number	Producer	Distributor	Number	Material	Measurements
glass flange, standard DN16	1340130160	Gebr. Rettberg GmbH, Rudolf- Wissell-Strasse 17, 37079, Göttingen, DE	see producer's adress	18	borosilicate glass	
KF clamping chain, type DN 10/16 KF	710653-1	"	"	18	synthetic	
KF tubulated reducing adapter	KF25R16A-40	Vacom, Vakuum Komponenten & Messtechnik GmbH, Gabelsbergerstrasse 9, 07749, Jena, DE	see producer's adress	1	aluminium	DN25 x DN16
KF bored flange	KF25B28-316	"	"	2	316 L stainless steel	DN 25
KF centering ring	KF25SVCR- 316	"	"	3	316 L stainless steel	DN 25
KF clamp ring	KF25C	"	"	3	aluminium	DN 25

Article description	Ordering number	Producer	Distributor	Number	Material	Measurements
KF flexible hose	FX25K100-316	Vacom, Vakuum Komponenten & Messtechnik GmbH, Gabelsbergerstrasse 9, 07749, Jena, DE	see producer's adress	1	316 L stainless steel, high flexible	DN 25, length 1000 mm, outer diameter 40 mm
KF bored flange	KF16B19-316	"	"	7	316 L stainless steel	DN16
KF centering ring	KF16SVCR-316	"	"	18	317 L stainless steel	DN16
KF clamp ring	KF16C	"	"	7	aluminium	DN16
KF flexible hose	FX16K100-304	"	"	6	304 stainless steel, high flexible	DN 16, length 1000 mm, outer diameter 30 mm
KF-Swagelok-adapter	KSWA1610	"	"	18	316 L stainless steel	DN 16, length 44 mm, outer diameter 30 mm, inner diameter 7.9 mm

Article description	Ordering number	Producer	Distributor	Number	Material	Measurements
lab-jack with adjusting wheel	GY/09118977	Rudolf Grauer AG, Taastrasse 12, 9113, Degersheim, CH	Th. Geyer GmbH & Co. KG, Dornier- strasse 4, 71272, Ren- ningen, DE	4	aluminium ano- dized	200 mm x 200 mm
teflon hose	741632	Fa. H. Riesbeck, Tau- nusstrasse 2, 63595, Biebergemünd, DE	see producer's adress	1	teflon	outer diameter 3.2 mm
vacuum manifold welded with 6 connec- tion tubes	hand-made	Fine mechanics, Fa- culty 07, Justus- Liebig-Universität Gießen, Heinrich- Buff-Ring 16, 35392, Gießen, DE	see producer's adress	1	316 L stainless steel	length connection tube 100 mm, outer diameter 10 mm, wall 1.5 mm
angular connection tube	"	"	"	6	316 L stainless steel	90° angle, tube outer diameter 10 mm, wall 1.5 mm, tube length (short side) 80 mm, tube length (long side) 100 mm
short connection tube	"	"	"	18	316 L stainless steel	outer diameter 10 mm, wall 1.5 mm, length 50 mm

Article description	Ordering number	Producer	Distributor	Number	Material	Measurements
test tube consisting of DN16 glass flange	hand-made	Glass blowing, Justus-Liebig-Universität Gießen, Heinrich-Buff-Ring 58, 35392, Gießen, DE	see producer's adress	6	borosilicate glass, heavy-walled	round-bottom, length 120 mm
U-tube consisting of DN16 glass flanges	"	"	"	6	borosilicate glass, heavy-walled	width 180 - 200.5 mm, length 180,5 - 200 mm, distance between U-tube arms 40.5 mm

8.2 Appendix 2

Table 9: Raw data of validation experiment 1.

$\delta^2\text{H}$ [‰]	$\delta^{18}\text{O}$ [‰]	sample type
-60.634	-8.742	Gießen's tap water original sample
-56.585	-8.913	"
-57.862	-9.216	"
-60.411	-8.814	"
-56.992	-9.240	"
-57.399	-9.327	Gießen's tap water without high-purity nitrogen aeration sample after extraction
-61.414	-8.774	"
-55.433	-9.287	"
-57.823	-9.329	"
-56.590	-9.499	"
-57.297	-9.740	"
-58.367	-9.365	"
-58.183	-9.332	"
-55.616	-9.757	"
-55.792	-9.927	"
-61.447	-8.593	"
-56.576	-9.636	"

Table 10: Raw data of validation experiment 2.1.

$\delta^2\text{H}$ [‰]	$\delta^{18}\text{O}$ [‰]	sample type
-57.399	-9.327	Gießen's tap water without high-purity nitrogen aeration sample after extraction
-61.414	-8.774	"
-55.433	-9.287	"
-57.823	-9.329	"
-56.590	-9.499	"
-57.297	-9.740	"
-58.367	-9.365	"
-58.183	-9.332	"
-55.616	-9.757	"
-55.792	-9.927	"
-61.447	-8.593	"
-56.576	-9.636	"
-59.258	-9.421	Gießen's tap water with high-purity nitrogen aeration sample after extraction
-57.569	-9.282	"
-58.980	-9.330	"
-58.611	-9.356	"
-58.065	-9.452	"
-59.136	-9.268	"
-57.994	-9.119	"
-57.775	-9.286	"

Table 11: Raw data of validation experiment 2.2.

$\delta^2\text{H}$ [‰]	$\delta^{18}\text{O}$ [‰]	sample type
-57.141	-8.020	Schwingbach water original sample
-54.651	-8.422	"
-54.233	-8.776	"
-57.967	-8.305	"
-56.501	-8.772	"
-55.098	-9.031	Schwingbach water with high-purity nitrogen aeration sample after extraction
-55.796	-8.977	"
-55.653	-9.173	"
-55.698	-8.886	"
-54.394	-9.061	"
-54.704	-8.799	"
-55.220	-8.520	"
-54.814	-8.774	"
-56.040	-8.541	"
-55.657	-8.597	"
-55.301	-8.485	"
-57.833	-8.239	"

Table 12: Raw data of validation experiment 3.

$\delta^2\text{H}$ [‰]	$\delta^{18}\text{O}$ [‰]	sample type
-1.793	-1.282	Precipitation from Gießen with high-purity nitrogen aeration sample after extraction
-1.135	-1.286	"
-1.504	-1.368	"
-1.791	-1.274	"
-1.263	-1.610	"
-1.363	-1.108	"
-56.098	-9.059	Schwingbach water with high-purity nitrogen aeration sample after extraction
-56.023	-9.161	"
-58.419	-8.429	"
-55.627	-9.181	"
-57.408	-8.681	"
-56.561	-8.866	"